NASA Technical Memorandum 4643

Predictions of Thermal Buckling Strengths of Hypersonic Aircraft Sandwich Panels Using Minimum Potential Energy and Finite Element Methods

William L. Ko

May 1995

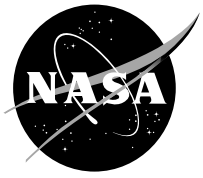

NASA Technical Memorandum 4643

Predictions of Thermal Buckling Strengths of Hypersonic Aircraft Sandwich Panels Using Minimum Potential Energy and Finite Element Methods

William L. Ko
Dryden Flight Research Center
Edwards, California

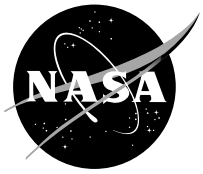

National Aeronautics and
Space Administration

Office of Management

Scientific and Technical
Information Program

1995

CONTENTS

PAGE

ABSTRACT 1

NOMENCLATURE 1

INTRODUCTION 3

DESCRIPTION OF PROBLEM 4

RAYLEIGH–RITZ THERMAL BUCKLING ANALYSIS 4
- Panel Boundary Conditions 4
- Deformation Functions 5
- Thermal Buckling Equations 6

FINITE ELEMENT THERMAL BUCKLING ANALYSIS 9
- Finite Element Modeling 9
- Eigenvalue Extractions 10

NUMERICAL EXAMPLES 11

RESULTS 12
- Eigenvalue Iterations 12
- Buckling Temperatures 13

CONCLUSIONS 14

APPENDIX A—COEFFICIENTS OF CHARACTERISTIC EQUATIONS 30

APPENDIX B—BUCKLING EQUATIONS 39

REFERENCES 48

TABLES

1. Sizes of three finite element models A, B, and C (c.f., fig. 6) 10

2. Buckling temperatures of sandwich panels calculated using minimum energy and finite element models 13

FIGURES

1. Rectangular honeycomb-core sandwich panel 15

2. Rectangular sandwich panel under thermal loading 15

3. Four types of edge conditions 16

4. Edge distortions of sandwich panel under different edge conditions; no edge distortions for 4C condition 17

5. Quarter-panel and half-panel regions for finite element models. 18
6. Three finite element models generated for sandwich panels of different aspect ratios 19
7. Modeling of sandwich panel. 20
8. Simulation of different edge conditions 21
9. Convergence curves of eigenvalue iterations; 4C condition; $b/a = 1$ 22
10. Increase of processor time with number of eigenvalue iterations; ELXSI 6400 computer 22
11. Buckled shapes of $b/a = 1$ sandwich panel under different edge conditions; half panel. 23
12. Buckled shapes of $b/a = 2$ sandwich panel under different edge conditions; full panel 25
13. Buckled shapes of $b/a = 3$ sandwich panel under different edge conditions; half panel. 27
14. Buckling temperature curves for titanium sandwich panels under different edge conditions; a = constant 29

ABSTRACT

Thermal buckling characteristics of hypersonic aircraft sandwich panels of various aspect ratios were investigated. The panel is fastened at its four edges to the substructures under four different edge conditions and is subjected to uniform temperature loading. Minimum potential energy theory and finite element methods were used to calculate the panel buckling temperatures. The two methods gave fairly close buckling temperatures. However, the finite element method gave slightly lower buckling temperatures than those given by the minimum potential energy theory. The reasons for this slight discrepancy in eigensolutions are discussed in detail. In addition, the effect of eigenshifting on the eigenvalue convergence rate is discussed.

NOMENCLATURE

A_{mn}, A_{kl}	Fourier coefficients of trial function for *w*, in.
$\bar{A}_{ij}$	extensional stiffnesses of sandwich panel, $\bar{A}_{11} = \frac{2t_s E_x}{1-\nu_{xy}\nu_{yx}}$, $\bar{A}_{12} = \frac{2t_s \nu_{yx} E_x}{1-\nu_{xy}\nu_{yx}}$ $\bar{A}_{21} = \frac{2t_s \nu_{xy} E_y}{1-\nu_{xy}\nu_{yx}}$, $\bar{A}_{22} = \frac{2t_s E_y}{1-\nu_{xy}\nu_{yx}}$, $\bar{A}_{66} = 2t_s G_{xy}$, lb/in
a	length of sandwich panel, in.
a^{ij}_{mnkl}	coefficients of characteristic equations
b	width of sandwich panel, in.
B_{mn}, B_{kl}	Fourier coefficients of trial function for γ_{xz}, in/in
c	shift factor in eigenvalue extractions
C_{mn}, C_{kl}	Fourier coefficients of trial function for γ_{yz}, in/in
D_{ij}	bending stiffnesses of sandwich panel, $D_{11} = \frac{2E_x I_s}{1-\nu_{xy}\nu_{yx}}$, $D_{12} = \frac{2\nu_{yx} E_x I_s}{1-\nu_{xy}\nu_{yx}}$ $D_{21} = \frac{2\nu_{xy} E_y I_s}{1-\nu_{xy}\nu_{yx}}$, $D_{22} = \frac{2E_y I_s}{1-\nu_{xy}\nu_{yx}}$, $D_{66} = 2G_{xy} I_s$, in–lb
D_{Qx}, D_{Qy}	transverse shear stiffnesses in *xz*-, *yz*-planes, $D_{Qx} = h_c G_{cxz}$, $D_{Qy} = h_c G_{cyz}$, lb/in
D^*	flexural stiffness parameter, $\sqrt{D_{11}D_{22}}$, in–lb
d_1, d_2, d_3	relative displacements of actual face sheets in *x*-, *y*-, and *z*-directions, in.
d'_1, d'_2, d'_3	relative displacements of finite element face sheets in *x*-, *y*-, and *z*-directions, in.
E_{cx}, E_{cy}, E_{cz}	effective Young's moduli of honeycomb core, lb/in^2
E_x, E_y	Young's moduli of face sheets, lb/in^2
E'_{cz}	effective Young's modulus of finite element sandwich core in z-direction, lb/in^2
G_{cxy}, G_{cxz}, G_{cyz}	effective shear moduli of honeycomb core, lb/in^2

G'_{cxz}, G'_{cyz}	effective transverse shear moduli of finite element sandwich core, lb/in^2
G_{xy}	shear modulus of face sheets, lb/in^2
h	depth of sandwich panel = distance between middle planes of two face sheets, in.
h_c	depth of honeycomb core, $h_c = h - t_s$, in.
i	index, 1, 2, 3, …
I_s	moment of inertia, per unit width, of a face sheet taken with respect to horizontal centroidal axis of the sandwich panel, $I_s = \frac{1}{4}t_s h^2 + \frac{1}{12}t_s^3$, in^4/in
j	index, 1, 2, 3, …
JLOC	joint location (used in figures and tables)
K	system stiffness matrix
k	index, 1, 2, 3, …
K_g	system initial stress stiffness matrix corresponding to a particular applied force condition
k_x, k_y	compressive buckling load factors in x- and y-directions, $k_x = \frac{N_x^T a^2}{\pi^2 D^*}$, $k_y = \frac{N_y^T a^2}{\pi^2 D^*}$
k_{xy}	shear buckling load factor, $k_{xy} = \frac{N_{xy}^T a^2}{\pi^2 D^*}$
l	index, 1, 2, 3, …
m	number of buckle half waves in x-direction
M_x, M_y	bending moment intensities, (in–lb)/in
n	number of buckle half waves in y-direction
N_x^T, N_y^T, N_{xy}^T	thermal forces, lb/in
SPAR	structural performance and resizing finite element computer program
t_s	thickness of sandwich face sheets, in.
u, v, w	displacement components in x-, y-, and z-directions, respectively, in.
X	displacement vector
x, y, z	rectangular Cartesian coordinates
x_G, y_G	global x- and y-coordinates for finite element model
α_x, α_y	coefficients of thermal expansion, in/in-°F
α_{xy}	coefficients of thermal shear distortion, in/in-°F
γ_{xz}, γ_{yz}	transverse shear strain in xz- and yz-planes, in/in
ΔT	temperature rise, °F
ΔT_a	assumed buckling temperature, °F

ΔT_{cr}	critical buckling temperature, °F
ζ	numerical coefficient of N_y^T in a_{mnkl}^{11}
η	numerical factor in buckling equation, which changes with the edge condition
λ_i	eigenvalue of *i*-th buckling mode
ν_{xy}, ν_{yz}	Poisson ratios of face sheets, also used for those of sandwich panel
ν_{cxy}, ν_{cyz}, ν_{cxz}	Poisson ratios of honeycomb core
ξ	numerical coefficient of N_x^T in a_{mnkl}^{11}
ρ_{Hc}	specific weight of titanium honeycomb core, lb/in^3
ρ_{Ti}	specific weight of titanium material, lb/in^3

INTRODUCTION

Hypersonic aircraft structural panels are subjected not only to aerodynamic loading (mechanical loading), but also to aerodynamic heating (thermal loading). These structural panels are usually called hot structural panels because they operate at elevated temperatures. For certain cases, the thermal load could be the primary load, and therefore, it could be a key factor in the design of the hot structures. When a monolithic hot structure is subjected to uniform temperature field and is allowed to expand freely, no thermal stresses can be generated in the structural panel. When the temperature field is nonuniform, thermal stresses can build up in the panel even if it can expand freely. In actual applications, the structural panels are attached to relatively cooler substructures (i.e., spars and ribs, both of which act as heat sinks); the panels are, therefore, constrained from free expansion. These constraints will cause thermal stresses to build up in the panels. The heating over an individual panel surface is usually relatively uniform; however, the panel surface temperatures are seldom uniform over the entire panel surface because the panel edges are attached to the heat sinks (i.e., relatively cooler substructures). The temperature rise over the panel surface will then have a plateau in a large central region and will taper down near the cooler edges. That is, the temperature rise profile over the panel surface will look like a truncated dome shape. High-intensity thermal loading could induce (1) thermal buckling, (2) material degradation, (3) thermal creep, (4) thermal yielding, (5) thermal cracking after cooling down, etc. Excess thermal deformation caused by thermal buckling could disturb the airflow field, creating localized hot spots that could degrade the panel's structural performance.

When the structural panels are applied as the hypersonic aircraft wing skins, the aerodynamic loading during hypersonic flight will cause the wing upper panels to be under combined spanwise compression (resulting from wing bending) and shear (resulting from wing torsion). On the other hand, the wing lower skin panels will be subjected to combined spanwise tension and shear loading. Under thermal loading, both the wing upper and lower skin panels will be under mainly biaxial compression with certain localized shear. The thermal loading will increase the mechanical compressive stresses in the wing upper panels, and tend to reduce the mechanical compressive stresses in the wing lower panels. Thus, the thermomechanical buckling characteristics of the hot structural panels are a critical concern in the hypersonic aircraft wing structural panels.

Thermal buckling problems of single plates (continuous or laminated composites) were investigated by several authors in recent years (refs. 1–6), and thermomechanical buckling characteristics of the hot structural sandwich panels were analyzed extensively by Ko and Jackson (refs. 7–12). Using the minimum potential energy method, Ko and Jackson developed thermomechanical buckling equations for orthotropic rectangular sandwich panels subjected to combined mechanical compressive and shear loading, or under thermal loading (refs. 11–12).

This report investigates the thermal buckling characteristics of uniformly heated rectangular titanium sandwich panels of different aspect ratios supported under four different edge conditions. The thermal buckling loads (or buckling temperatures) will be calculated using Ko–Jackson thermal buckling equations (refs. 11–12) and the finite element method for the purpose of validating the Ko-Jackson theory. The thermal buckling solutions obtained from the two methods will be compared and their discrepancies discussed.

DESCRIPTION OF PROBLEM

Figure 1 shows the geometry of the hypersonic aircraft rectangular sandwich panel. The sandwich panel has length a, width b, and depth h. It is fabricated with titanium face sheets of the same thicknesses t_s, joined together through a titanium honeycomb core of depth h_c using the enhanced diffusion bonding process (ref. 13). Figure 2 shows the combined thermal forces acting on the middle plane of the sandwich panel.

For the thermal buckling analysis, the panel will be subjected to uniform temperature field under four different edge conditions shown in figure 3. The edges in the x- and y-directions are defined, respectively, as sides and ends. The minimum potential energy thermal buckling theory developed by Ko and Jackson (refs. 11–12) and the finite element method will be used to calculate panel buckling temperatures, and the eigensolutions based on the two methods will be compared.

RAYLEIGH–RITZ THERMAL BUCKLING ANALYSIS

In the thermal buckling analysis of sandwich panels conducted by Ko and Jackson (refs. 11–12), the extensional and bending stiffnesses are provided by the two face sheets, and the panel transverse shear stiffness is provided by the sandwich core only.

Panel Boundary Conditions

The four sets of boundary conditions used in the Ko and Jackson thermal buckling analysis (refs. 11–12) are given below.

Case 1: Four edges simply supported (4S condition)

$$x = 0, a: \quad u = v = w = M_x = \gamma_{yz} = 0 \tag{1}$$

$$y = 0, b: \quad u = v = w = M_y = \gamma_{xz} = 0 \tag{2}$$

Case 2: Four edges clamped (4C condition)

$$x = 0, a: \quad u = v = w = \frac{\partial w}{\partial x} = \gamma_{xz} = \gamma_{yz} = 0 \tag{3}$$

$$y = 0, b: \quad u = v = w = \frac{\partial w}{\partial y} = \gamma_{xz} = \gamma_{yz} = 0 \tag{4}$$

Case 3: Two sides clamped, two ends simply supported (2C2S condition)

$$x = 0, a: \quad u = v = w = M_x = \gamma_{yz} = 0 \tag{5}$$

$$y = 0, b: \quad u = v = w = \frac{\partial w}{\partial y} = \gamma_{xz} = \gamma_{yz} = 0 \tag{6}$$

Case 4: Two sides simply supported, two ends clamped (2S2C condition)

$$x = 0, a: \quad u = v = w = \frac{\partial w}{\partial x} = \gamma_{xz} = \gamma_{yz} = 0 \tag{7}$$

$$y = 0, b: \quad u = v = w = M_y = \gamma_{xz} = 0 \tag{8}$$

For anisotropic sandwich panels, cases 3 and 4 will give different thermal buckling solutions.

Deformation Functions

For satisfying the different sets of boundary conditions (1) through (8), the associated deformation functions $\{w, \gamma_{xz}, \gamma_{yz}\}$ chosen by Ko and Jackson (refs. 11–12) in the thermal buckling analysis of the sandwich panels have the following forms:

Case 1: 4S condition

$$w(x, y) = \sum_{m=1}^{\infty} \sum_{n=1}^{\infty} A_{mn} \sin\frac{m\pi x}{a} \sin\frac{n\pi y}{b} \tag{9}$$

$$\gamma_{xz}(x, y) = \sum_{m=1}^{\infty} \sum_{n=1}^{\infty} B_{mn} \cos\frac{m\pi x}{a} \sin\frac{n\pi y}{b} \tag{10}$$

$$\gamma_{yz}(x, y) = \sum_{m=1}^{\infty} \sum_{n=1}^{\infty} C_{mn} \sin\frac{m\pi x}{a} \cos\frac{n\pi y}{b} \tag{11}$$

Case 2: 4C condition

$$w(x, y) = \sin\frac{\pi x}{a} \sin\frac{\pi y}{b} \sum_{m=1}^{\infty} \sum_{n=1}^{\infty} A_{mn} \sin\frac{m\pi x}{a} \sin\frac{n\pi y}{b} \tag{12}$$

$$\begin{aligned} \gamma_{xz}(x, y) = {} & \cos\frac{\pi x}{a} \sin\frac{\pi y}{b} \sum_{m=1}^{\infty} \sum_{n=1}^{\infty} B_{mn} \sin\frac{m\pi x}{a} \sin\frac{n\pi y}{b} \\ & + \sin\frac{\pi x}{a} \sin\frac{\pi y}{b} \sum_{m=1}^{\infty} \sum_{n=1}^{\infty} m B_{mn} \cos\frac{m\pi x}{a} \sin\frac{n\pi y}{b} \end{aligned} \tag{13}$$

$$\begin{aligned} \gamma_{yz}(x, y) = {} & \sin\frac{\pi x}{a} \cos\frac{\pi y}{b} \sum_{m=1}^{\infty} \sum_{n=1}^{\infty} C_{mn} \sin\frac{m\pi x}{a} \sin\frac{n\pi y}{b} \\ & + \sin\frac{\pi x}{a} \sin\frac{\pi y}{b} \sum_{m=1}^{\infty} \sum_{n=1}^{\infty} n C_{mn} \sin\frac{m\pi x}{a} \cos\frac{n\pi y}{b} \end{aligned} \tag{14}$$

Case 3: 2C2S condition

$$w(x,y) = \sin\frac{\pi y}{b}\sum_{m=1}^{\infty}\sum_{n=1}^{\infty} A_{mn}\sin\frac{m\pi x}{a}\sin\frac{n\pi y}{b} \tag{15}$$

$$\gamma_{xz}(x,y) = \sin\frac{\pi y}{b}\sum_{m=1}^{\infty}\sum_{n=1}^{\infty} B_{mn}\cos\frac{m\pi x}{a}\sin\frac{n\pi y}{b} \tag{16}$$

$$\begin{aligned}\gamma_{yz}(x,y) = {} & \cos\frac{\pi y}{b}\sum_{m=1}^{\infty}\sum_{n=1}^{\infty} C_{mn}\sin\frac{m\pi x}{a}\sin\frac{n\pi y}{b} \\ & + \sin\frac{\pi y}{b}\sum_{m=1}^{\infty}\sum_{n=1}^{\infty} nC_{mn}\sin\frac{m\pi x}{a}\cos\frac{n\pi y}{b}\end{aligned} \tag{17}$$

Case 4: 2S2C condition

$$w(x,y) = \sin\frac{\pi x}{a}\sum_{m=1}^{\infty}\sum_{n=1}^{\infty} A_{mn}\sin\frac{m\pi x}{a}\sin\frac{n\pi y}{b} \tag{18}$$

$$\begin{aligned}\gamma_{xz}(x,y) = {} & \cos\frac{\pi x}{a}\sum_{m=1}^{\infty}\sum_{n=1}^{\infty} B_{mn}\sin\frac{m\pi x}{a}\sin\frac{n\pi y}{b} \\ & + \sin\frac{\pi x}{a}\sum_{m=1}^{\infty}\sum_{n=1}^{\infty} mB_{mn}\cos\frac{m\pi x}{a}\sin\frac{n\pi y}{b}\end{aligned} \tag{19}$$

$$\gamma_{yz}(x,y) = \sin\frac{\pi x}{a}\sum_{m=1}^{\infty}\sum_{n=1}^{\infty} C_{mn}\sin\frac{m\pi x}{a}\cos\frac{n\pi y}{b} \tag{20}$$

The choice of these four sets of deformation functions, each of which satisfies the associated boundary conditions (1) through (8), is for the mathematical amenability of the eigenvalue solutions. As shown in figure 4, the zero transverse shear distortions (i.e., $\gamma_{xz} = 0$ or $\gamma_{yz} = 0$) at the panel edges cannot be enforced simultaneously in the actual panel deformations, except for the 4C condition.

Thermal Buckling Equations

The thermal buckling equations developed by Ko and Jackson (refs. 11–12) for uniformly heated and constrained rectangular orthotropic sandwich panels using the Rayleigh–Ritz method, written in terms of temperature rise ΔT for each set of integral values $\{m, n\}$ (or mode shape), have the following form

$$\sum_k\sum_l\left[\frac{M_{mnkl}}{\Delta T} + P_{mnkl} + \delta_{mnkl}\right]A_{kl} = 0 \tag{21}$$

The bending-stiffness parameter M_{mnkl} and the extensional stiffness parameter P_{mnkl} in equation (21) are defined as

$$M_{mnkl} \equiv \frac{ab}{\eta \bar{A}_{66}\alpha_{xy}} \left[\underbrace{a^{-11}_{mnkl}}_{\substack{\text{classical}\\ \text{thin plate}\\ \text{theory term}}} + \underbrace{\frac{a^{12}_{mnkl}(a^{23}_{mnkl}a^{31}_{mnkl} - a^{21}_{mnkl}a^{33}_{mnkl}) + a^{13}_{mnkl}(a^{21}_{mnkl}a^{32}_{mnkl} - a^{22}_{mnkl}a^{31}_{mnkl})}{a^{22}_{mnkl}a^{33}_{mnkl} - a^{23}_{mnkl}a^{32}_{mnkl}}}_{\text{transverse shear effect terms}} \right] \tag{22}$$

$$P_{mnkl} \equiv \frac{ab}{\eta \bar{A}_{66}\alpha_{xy}} [\xi(m, k)(\bar{A}_{11}\alpha_x + \bar{A}_{12}\alpha_y) + \zeta(n, l)(\bar{A}_{21}\alpha_x + \bar{A}_{22}\alpha_y)] \tag{23}$$

The characteristic coefficients a^{ij}_{mnkl} $(i, j = 1, 2, 3)$ appearing in equation (22) are defined in appendix A, and a^{-11}_{mnkl} in equation (22) is the first part of a^{11}_{mnkl}, containing no thermal loading terms (i.e., terms containing $\{k_x, k_y\}$). The parameters $\{\xi, \zeta\}$ in equation (23) are, respectively, the numerical coefficients of the load factors $\{k_x, k_y\}$ contained in a^{11}_{mnkl}. The values of $\{\xi, \zeta\}$ change with the indicial and edge conditions (ref. 12).

The numerical parameter η, appearing in equations (22) and (23), and the special delta function δ_{mnkl}, appearing in equation (21), are defined for different edge conditions as (ref. 12)

Case 1: 4S condition

$$\begin{cases} \eta = 32 \\ \delta_{mnkl} = \dfrac{mnkl}{(m^2 - k^2)(n^2 - l^2)}; \quad m \pm k = \text{odd}, \quad n \pm l = \text{odd} \end{cases} \tag{24}$$

Case 2: 4C condition

$$\begin{cases} \eta = \dfrac{(16)^3}{2} \\ \delta_{mnkl} = \dfrac{mnkl[m^2 + k^2 - 2][n^2 + l^2 - 2]}{(m^2 - k^2)(n^2 - l^2)[(m + k)^2 - 4][(m - k)^2 - 4][(n + l)^2 - 4][(n - l)^2 - 4]}; \quad m \pm k = \text{odd}, \; n \pm l = \text{odd} \end{cases} \tag{25}$$

Case 3: 2C2S condition

$$\begin{cases} \eta = 8^3 \\ \delta_{mnkl} = \dfrac{mnkl[2 - (n^2 + l^2)]}{(m^2 - k^2)(n^2 - l^2)[(n + l)^2 - 4][(n - l)^2 - 4]}; \quad m \pm k = \text{odd}, \; n \pm l = \text{odd} \end{cases} \tag{26}$$

Case 4: 2S2C condition

$$\begin{cases} \eta = 8^3 \\ \delta_{mnkl} = \dfrac{mnkl[2 - (m^2 + k^2)]}{(m^2 - k^2)(n^2 - l^2)[(m + k)^2 - 4][(m - k)^2 - 4]}; \quad m \pm k = \text{odd}, \; n \pm l = \text{odd} \end{cases} \tag{27}$$

In the thermal buckling equation (21), both M_{mnkl} and P_{mnkl} terms contain temperature dependent material properties. Thus, in the eigenvalue solution process using equation (21), one has to assume a buckling temperature ΔT_a and use the material properties corresponding to ΔT_a as inputs to calculate the buckling temperature ΔT_{cr}. This material property iteration process must continue until ΔT_a approaches ΔT_{cr}. Thus, in the thermal buckling, the eigenvalue solution process is a multi-step process. However, in the mechanical buckling, only one step eigenvalue solution process is required.

When the coefficient of thermal shear distortion is zero (i.e., $\alpha_{xy} = 0$), the buckling equation (21) takes on the form

$$\sum_k \sum_l \left[\frac{\overline{M}_{mnkl}}{\Delta T} + \bar{P}_{mnkl} \right] A_{kl} = 0 \tag{28}$$

where $\overline{M}_{mnkl}$ and $\bar{P}_{mnkl}$ are defined as

$$\overline{M}_{mnkl} \equiv \left[\bar{a}^{11}_{mnkl} + \frac{a^{12}_{mnkl}(a^{23}_{mnkl} a^{31}_{mnkl} - a^{21}_{mnkl} a^{33}_{mnkl}) + a^{13}_{mnkl} (a^{21}_{mnkl} a^{32}_{mnkl} - a^{22}_{mnkl} a^{31}_{mnkl})}{a^{22}_{mnkl} a^{33}_{mnkl} - a^{23}_{mnkl} a^{32}_{mnkl}} \right] \tag{29}$$

$$\bar{P}_{mnkl} \equiv [\xi(m, k)(\bar{A}_{11}\alpha_x + \bar{A}_{12}\alpha_y) + \zeta(n, l)(\bar{A}_{21}\alpha_x + \bar{A}_{22}\alpha_y)] \tag{30}$$

When equation (28) is reduced to the isotropic case with no transverse shear effects, the buckling temperature ΔT_{cr} will be independent of the material's modulus of elasticity (ref. 14).

The characteristic equation (21) forms a system of infinite number of simultaneous homogeneous equations, each of which is associated with each indicial combination of $\{m, n\}$. Those simultaneous equations, generated from equation (21), have the following characteristics. The first two terms $(M_{mnkl} / \Delta T + P_{mnkl})$ of equation (21) are nonzero only for the indicial conditions $\{m = k \text{ or } m - k = 2\}$ and $\{n = l \text{ or } n - l = 2\}$ based on the indicial constraints for a^{ij}_{mnkl} (appendix A). Thus, if $(m \pm n)$ is even, then $(k \pm l)$ is also even, and if $(m \pm n)$ is odd, then $(k \pm l)$ is also odd. The special delta function δ_{mnkl} in the third term of equation (21) is nonzero only when $(m \pm k)$ is odd and $(n \pm l)$ is odd. It follows that $(m \pm k) \pm (n \pm l) = (m \pm n) \pm (k \pm l) =$ even. This implies that if $(m \pm n)$ is even, then $(k \pm l)$ is also even, and if $(m \pm n)$ is odd, so also is $(k \pm l)$. Because of these indicial characteristics, there is no coupling between the even case (i.e., symmetric buckling) and the odd case (i.e., antisymmetric buckling). Thus, the simultaneous equations generated from equation (21) may be divided into two groups that are independent of each other—one group for which $(m \pm n)$ is even, and the other group for which $(m \pm n)$ is odd (refs. 11–12).

For the deflection coefficients A_{kl} to have nontrivial solutions for given aspect ratio b/a, the determinant of coefficients of unknown A_{kl} of the simultaneous homogeneous equations written out from equation (21) must vanish. The largest eigenvalue $1/\Delta T$ thus obtained will give the lowest buckling temperature ΔT_{cr}. The determinants of the coefficients of the simultaneous equations written out from equation (21) up to order 12 are given in appendix B for the cases $m \pm n =$ even (symmetric buckling) and $m \pm n =$ odd (antisymmetric buckling) for different edge conditions. The determinants of order 12 were found to give sufficiently accurate eigensolutions and, therefore, the determinants were truncated at order 12 in the present eigenvalue extractions. In appendix B one notices that for the 4S edge condition only, $(M_{mnkl} / \Delta T + P_{mnkl})$ terms form the diagonal terms of the determinants, and the nonzero off-diagonal terms consist only of numerical values given by δ_{mnkl}. However, for the rest of edge conditions, $(M_{mnkl} / \Delta T + P_{mnkl})$ not only appear in the diagonal terms, but also in the off-diagonal terms (mixed with the numerical terms associated with δ_{mnkl}).

FINITE ELEMENT THERMAL BUCKLING ANALYSIS

The structural performance and resizing (SPAR) finite element computer program (ref. 15) was used in the finite element thermal buckling analysis of the sandwich panels.

Finite Element Modeling

To gather thermal buckling data of sandwich panels having a wide range of aspect ratios b/a, three basic finite element models of different b/a were set up so that each model would cover certain limited range of b/a. Changing b/a of each model was accomplished by simply modifying length b and keeping length a constant. Sometimes more elements had to be added to an overstretched model to maintain proper element aspect ratios. An overstretched model without additional elements could result in local buckling of slender element cells rather than global buckling of the panels (i.e., local buckling temperature is less than the global buckling temperature). For low b/a (<1.8) and high b/a (>2.9) aspect ratio panels (figs. 5(a) and 5(c)) for which the lowest buckling mode were symmetric, only the quarter panels were modeled. The SPAR constraint commands SYMMETRY PLANE = 1 and SYMMETRY PLANE = 2 (ref. 15) were then used to generate the full panels. For moderate b/a ($1.8 \le b/a \le 2.9$) aspect ratio panels (fig. 5(b)) for which the lowest buckling mode could be either symmetric or antisymmetric, half panels were modeled. The SPAR constraints command SYMMETRY PLANE = 1 was then used to generate the full panels. For purely antisymmetric buckling, one can model only a quarter panel and use the constraint commands SYMMETRY PLANE = 1 and ANTISYMMETRY PLANE = 2 to generate the whole panel. However, such quarter-panel models were not used in gathering the buckling data because they consistently gave somewhat higher buckling temperatures than those given by the half-panel models. Figure 6 shows the three basic finite element models set up for the sandwich panels. Both models A and C are the quarter-panel models, but model B is a half-panel model. From these basic models, several modified models (not model shown) were also set up for handling certain aspect ratios and edge conditions.

Each face sheet of the sandwich panel was modeled with one layer of E43 elements (quadrilateral combined membrane and bending elements) and the sandwich core with one layer of S81 elements (hexahedron (or brick) elements), which connect the upper and the lower face-sheet elements E43. Because the joint locations of those face sheet elements E43 are located in the middle planes of the respective face sheets, the finite element core depth will then be h instead of the actual depth h_c (fig. 7). Thus, to simulate the actual relative displacements (or maintain same stiffness) between the two face sheets in the sandwich thickness direction and the x- and y-directions (i.e., $d_3 = d'_3$ and $d_1 = d'_1$ and $d_2 = d'_2$, fig. 7), the thickness elastic modulus E'_{cz}, and the transverse shear moduli G'_{cxz} and G'_{cyz} of the S81 elements had to be increased slightly according to the following relationships:

$$E'_{cz} = E_{cz}\frac{h}{h_c} \tag{31}$$

$$G'_{cxz} = G_{cxz}\frac{h}{h_c} \tag{32}$$

$$G'_{cyz} = G_{cyz}\frac{h}{h_c} \tag{33}$$

One can also model the sandwich core with one layer of S81 elements having the exact depth h_c, and then connect the gaps between E43 joints and S81 joints with rigid elements. However, this alternative modeling method requires twice as many total joint locations, and therefore, it was not used.

For simply supported edges, free rotation and free transverse shear deformation must be allowed (fig. 8(a)). To simulate this type of edge, pin-ended rigid rods were attached to the panel edge for connecting the two face sheets (sandwich core carries no extensional and bending stiffnesses), and then the midpoints of the rigid rods were pin-jointed to fix points lying in the sandwich middle plane (fig. 8(a)). Each pin-ended rigid rod was modeled with two identical E22 elements (beam element for which the intrinsic stiffness matrix is given). To simulate the rigidity of the rod, extensional and transverse shear stiffnesses of the E22 elements were made very large. The pin-joint condition at the face sheet edges was simulated by assigning zero values to the rotational spring constants in the stiffness matrix for the E22 elements. The pin-joint condition at the middle-plane fixed points was simulated by relaxing the three rotational constraints. Two methods were used to connect the ends of the E22 elements to the middle plane fixed points. In the first method (center drawing of fig. 8(a)), the first joint of each E22 element was connected to the associated joint of E43 element and its end point to the panel middle-plane fixed point. In the second method (right-hand drawing of fig. 8(a)), the ends of the two identical E22 elements, whose first joints were connected to the upper and the lower face sheets, were connected together to the middle-plane fixed point through E25 element (zero length element used to elastically connect geometrically coincidental joints). The stiffnesses of the E25 were made so large that the two E22 elements, connected together by the E25 element, will behave like one rigid rod. These two types of simply supported edge simulations were found to give identical thermal buckling solutions. In most of the buckling data gathering, the first edge simulation was used because it required less joint locations.

For the clamped edge (fig. 8(b)), the edges of the two face sheets were built into fixed vertical walls to generate the desired constraints of zero slope, zero in-plane displacements, and zero transverse shear deformations.

Table 1 shows the sizes of the three finite element models set up for the sandwich panels of different b/a.

Table 1. Sizes of three finite element models A, B, and C (c.f., fig. 6).

Feature	Model A	Model B	Model C
JLOC	2178	4850	4050
E43	2048	4608	3840
S81	1024	2304	1920

To make sure that the above finite element models gave accurate eigensolutions, the sandwich cores of model A was modified to two layers of S81 elements to investigate the eigensolution convergencies. It turned out that both the basic and the modified models gave practically identical eigensolutions. Because the modified model required about three times longer computational time, it was not used in the actual buckling data gatherings.

Eigenvalue Extractions

The eigenvalue equation for buckling problems is of the form

$$\lambda K_g X + KX = 0 \tag{34}$$

where

K_g = system initial stress stiffness matrix (or differential stiffness matrix), corresponding to particular applied force condition (e.g., thermal loading), and in general a function of X

K = system stiffness matrix

X = displacement vector

λ_i = eigenvalues for various buckling modes

The eigenvalues λ_i (i = 1,2,3,…) are the load factors by which the static load (mechanical or thermal) must be multiplied to produce buckling loads corresponding to various buckling modes. Namely, if the applied temperature load is ΔT, then the buckling temperature ΔT_{cr} for the i-th buckling mode is obtained from

$$\Delta T_{cr} = \lambda_i \Delta T \tag{35}$$

If it is desired to find eigenvalues in the neighborhood of c, then the following shifted eigenvalue equation may be used.

$$(\lambda - c)K_g X + (K + c\ K_g)X = 0 \tag{36}$$

In the eigenvalue extractions, the SPAR program uses an iterative process consisting of a Stodola matrix iteration procedure, followed by a Rayleigh–Ritz procedure, and then followed by a second Stodola procedure. This process results in successively refined approximations of i eigenvectors associated with the i eigenvalues of equation (34) closest to zero. Reference 15 describes the details of this process.

NUMERICAL EXAMPLES

The hot structural sandwich panels analyzed were fabricated with titanium face sheets and titanium sandwich core having the following geometrical and material properties.

Geometry:

$$a = 24 \text{ in.}$$
$$b = \text{varying}$$
$$h = 0.75 \text{ in.}$$
$$h_c = h - t_s = 0.69 \text{ in.}$$
$$t_s = 0.06 \text{ in.}$$

Material properties:

Face sheets

	70 °F	900 °F*
$E_x = E_y$, lb/in^2	16×10^6	13.1×10^6
G_{xy}, lb/in^2	6.2×10^6	5.0×10^6
$\nu_{xy} = \nu_{yx}$	0.31	0.31
$\alpha_x = \alpha_y$, in/in-°F	4.85×10^{-6}	5.35×10^{-6}
α_{xy}, in/in-°F	0	0
ρ_{Ti}, lb/in^3	0.16	0.16

*Mach 15 flight temperature.

Honeycomb core (properties at 600 °F)		
E_{cx}	=	2.7778×10^{4} lb/in^2
E_{cy}	=	2.7778×10^{4} lb/in^2
E_{cz}	=	2.7778×10^{5} lb/in^2
G_{cxy}	=	0.00613 lb/in^2
G_{cyz}	=	0.81967×10^{5} lb/in^2
G_{cxz}	=	1.81×10^{5} lb/in^2
ν_{cxy}	=	0.658×10^{-2}
ν_{cyz}	=	0.643×10^{-6}
ν_{cxz}	=	0.643×10^{-6}
$\alpha_x = \alpha_y$	=	5.37×10^{-6} in/in-°F
α_{xy}	=	0 in/in-°F
ρ_{Hc}	=	3.674×10^{-3} lb/in^3

The main objective of the present report is to study the general trend of thermal buckling characteristics of sandwich panels under different edge conditions, and to validate Ko-Jackson theory (ref. 12). Because of the lack of material property data at high temperatures, the material iteration process was not performed, and the face sheet properties at 900 °F and sandwich core properties at 600 °F were used in the buckling temperature calculations.

RESULTS

Eigenvalue Iterations

In finite element eigenvalue extractions, the maximum number of iterations was set to be 100. For most cases (with or without eigenshifting), however, the eigenvalues converged well below 100 iterations based on the convergence criterion ($| \lambda_i - \lambda_{i-1} | / \lambda_i) < 10^{-4}$. Figure 9 compares the convergence curves of eigenvalue iterations with and without shifting for the square panel ($b/a = 1$) under the 4C condition. With shifting, the number of iterations could be reduced from 14 to 9 iterations. For certain cases, the number of eigenvalue iterations with shifting turned out to be very close or even identical to that without shifting. For certain problems, such as the thermocryogenic buckling of cryogenic tanks (ref. 16), eigenshifting could drastically reduce the number of eigenvalue iterations (i.e., reduction in computer time). For the present sandwich panel buckling problem, however, the reduction in the number of eigenvalue iterations through the eigenshifting turned out to be relatively small or negligible.

In most of the thermal buckling data gathering, the eigenshifting method was used. The shifting factors used were near the values of the buckling temperatures predicted from the energy theory. In figure 10 the ELXSI 6400 computer processor times are plotted as functions of the number of eigenvalue iterations for the four edge conditions. The processor time per iteration (i.e., slope of the data fitting line) for the 4S, 4C, 2C2S, and 2S2C conditions are, respectively, 2.45, 1.88, 2.48, and 2.06 minutes.

Buckling Temperatures

Figures 11, 12, and 13, respectively, show the lowest-mode buckling shapes of sandwich panels of aspect ratios b/a = 1, 2, and 3 under the four different edge conditions. Notice that at the simply supported edges of the 4S case and at the clamped edges of the 2C2S and 2S2C cases, the transverse shear deformations cannot be zero (fig. 4). At higher b/a (figs. 12 and 13), the 4C and 2S2C cases required finer element models for obtaining global buckling. The square panel (b/a = 1, fig. 11), under all the four different edge conditions, buckled symmetrically with {m = 1, n = 1} buckling mode. For the b/a = 2 rectangular panel (fig. 12), the 4S, 4C and 2C2S conditions still induced symmetrical buckling mode of {m = 1, n = 1}. However, under the 2S2C condition, the rectangular panel buckled antisymmetrically under {m = 1, n = 2} buckling mode. For the slender panel of b/a = 3 (fig. 13), both 4S and 2C2S conditions continued to induce symmetrical buckling mode of {m = 1, n = 1}. However, under the 4C and 2S2C conditions, the multiple symmetrical buckling mode of {m = 1, n = 3} turned out to be the lowest buckling mode. In figure 14 the thermal buckling temperatures calculated using the minimum energy method (solid curves) and the finite element method (circular symbols) are plotted as functions of panel aspect ratio b/a for the four cases of edge conditions. Notice that for the high values of b/a, the thermal buckling solutions for the 2C2S and 2S2C cases approach those of the 4S and 4C cases, respectively, because the constraint effects of the shorter edges of the slender panels diminish. The buckling solutions obtained from the two methods compare fairly well. The average solution difference between the two methods are 3.87%, 1.62%, 2.04% and 2.71% respectively for the 4S, 4C, 2C2S and 2S2C cases. The finite element method tends to give slightly lower buckling temperatures than those given by the minimum-energy method. The reason could be the following: (1) the finite element method allows deformations in the sandwich thickness direction, which the minimum energy theory ignores, (2) the theoretical edge conditions of zero γ_{xz} and γ_{yz} (eqs. (1), (2), (5)–(8)) cannot be enforced properly in the finite element edge constraints for the 4S, 2C2S, and 2S2C conditions (fig 4), and (3) the finite element modeling assumptions. For the 4C case only, all the theoretical edge conditions could be enforced in the finite element edge constraints. For 4S, 4C and 2C2S cases, the discrepancy of the eignsolutions between the two methods is larger at the low values of b/a, and gradually diminishes at high values of b/a. This solution discrepancy is minimum for the 4C case, and maximum for the 4S case (because both γ_{xz} and γ_{yz} cannot be zero at the edges of the finite element modes). For the 2S2C case, the solution discrepancy is almost unaffected by the change of b/a. Table 2 lists the buckling temperatures ΔT_{cr} calculated from the minimum energy and the finite element methods.

Table 2. Buckling temperatures of sandwich panels calculated using minimum energy and finite element models.

	ΔT_{cr}, °F							
	4S		4C		2C2S		2S2C	
b/a	Energy theory	Finite element	Energy theory	Finite element	Energy theory	Finite element	Energy theory	Finite element
0.5	1297	1207	2541	2498	2424	2366	1512	1464
0.6	1051	970	2169	2126	1995	1938	1334	1286
0.7	885	815	1889	1847	1654	1603	1232	1187
0.8	769	710	1683	1645	1387	1343	1175	1132
0.9	682	637	1535	1499	1181	1143	1144	1105
1.0	622	583	1428	1396	1021	988	1128	1093
1.1	575	547	1352	1322	897	866	1122	1090
1.2	538	513	1297	1271	799	774	1121	1092
1.4	486	465	1232	1209	662	640	1126	1102
1.6	451	436	1199	1179	573	560	1136	1116

Table 2. Concluded.

	ΔT_{cr}, °F							
	4S		4C		2C2S		2S2C	
b/*a*	Energy theory	Finite element	Energy theory	Finite element	Energy theory	Finite element	Energy theory	Finite element
1.8	427	416	1183	1165	514	504	1144	1130
2.0	409	403	1175	1160	473	471	1128	1096
2.2	396	391	1172	1158	444	439	1122	1092
2.4	386	382	1171	1156	423	419	1121	1094
2.6	379	376	1164	1155	407	404	1122	1099
2.8	372	370	1156	1151	395	393	1126	1100
3.0	367	366	1150	1145	386	384	1128	1095
4.0	353	348	1140	1121	360	360	1124	1100

CONCLUSIONS

Thermal buckling characteristics of hypersonic aircraft honeycomb-core sandwich panels subjected to uniform temperature loading were analyzed using minimum energy theory and finite element methods. The thermal buckling curves were generated for titanium sandwich panels of various aspect ratios. The two methods predicted very close buckling temperatures, and thus, the Ko-Jackson theory was validated. The finite element method tended to give slightly lower buckling temperatures than those given by the minimum energy theory. The slight discrepancies in the eigensolutions between the two methods could be attributed to the following:

1. The minimum energy theory does not consider deformations in the panel thickness direction, whereas the finite element method does.
2. The theoretical zero transverse shear deformations at the panel edges cannot be enforced in the finite element models with simply supported edges and cannot be enforced simultaneously in the finite elements models with mixed simply supported and clamped edges.
3. Assumptions made in finite element modeling.

The discrepancy of the eigensolutions between the minimum energy theory and the finite element method is the largest for the simply supported edge condition, because the zero transverse shear deformations at the panel edges cannot be constrained in the finite element models. This solution discrepancy is larger at low values of *b*/*a* and gradually decreases as *b*/*a* increases. For the sandwich panels the eigenshifting has small effect on the improvement of the eigenvalue convergence rate.

The author gratefully acknowledges the contribution of the late Raymond H. Jackson, NASA mathematician, in setting up computer programs for the eigenvalue extractions.

Dryden Flight Research Center
National Aeronautics and Space Administration
Edwards, California, June 14, 1994

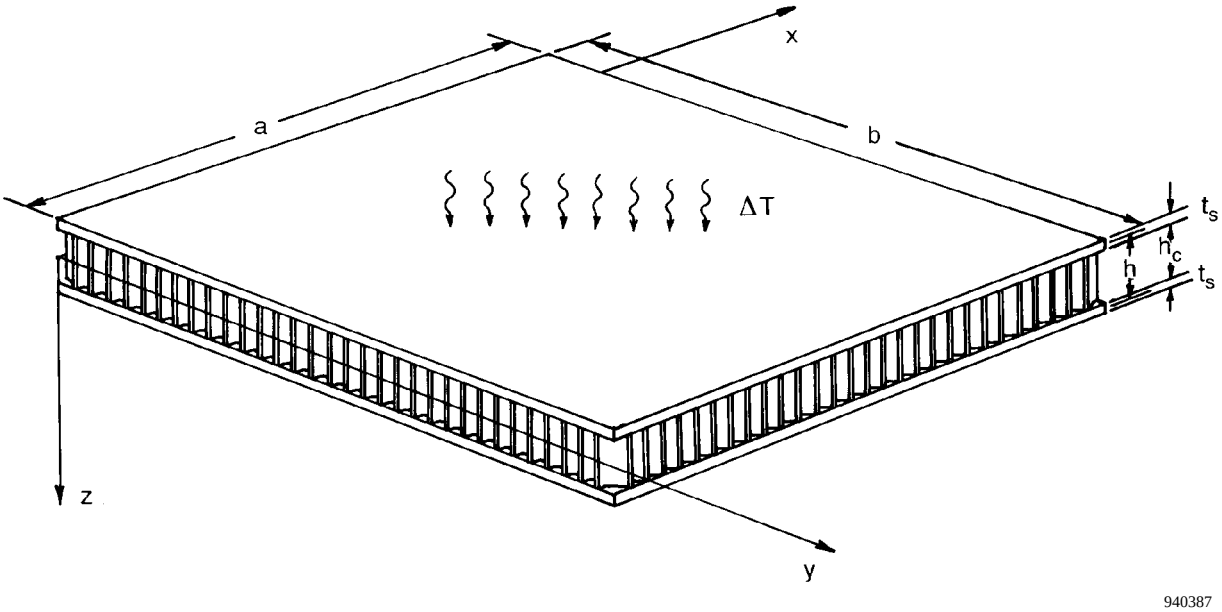

Figure 1. Rectangular honeycomb-core sandwich panel.

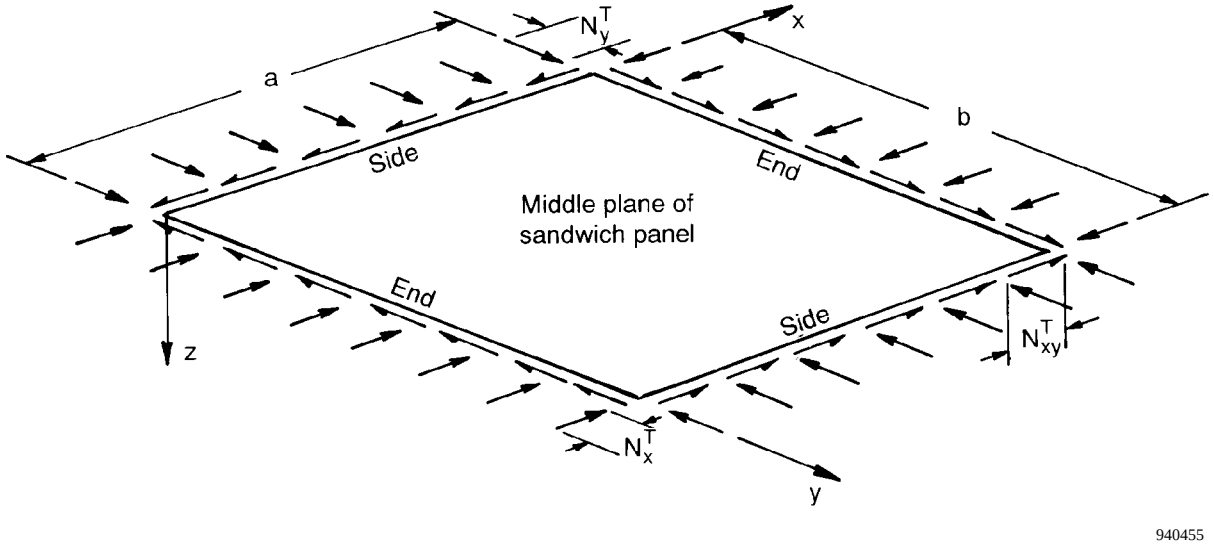

Figure 2. Rectangular sandwich panel under thermal loading.

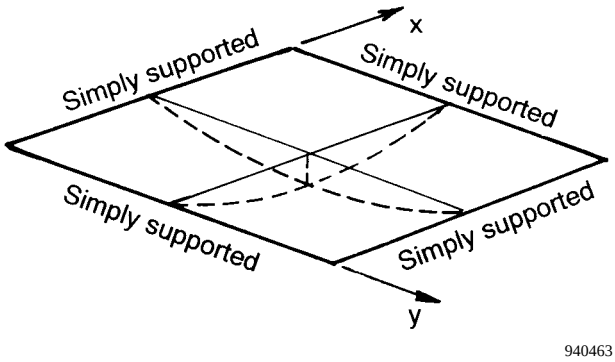

(a) Four edges simply supported (4S condition).

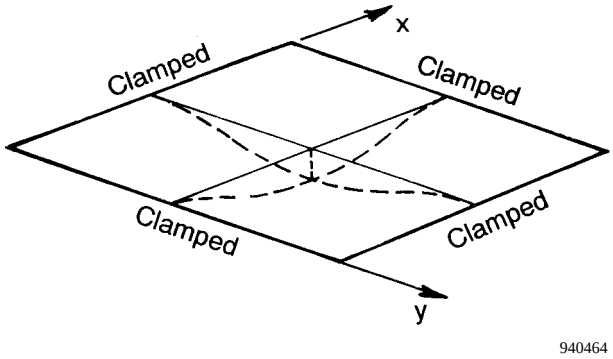

(b) Four edges clamped (4C condition).

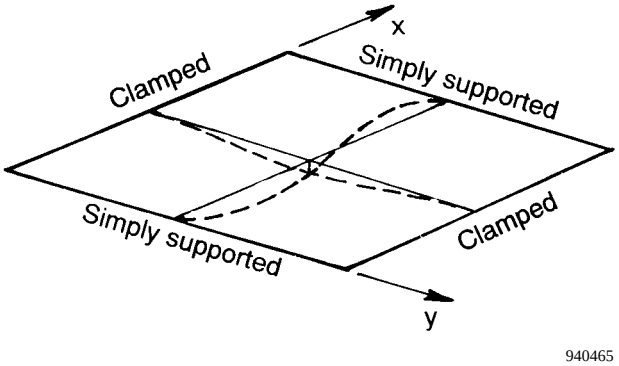

(c) Two sides clamped, two ends simply supported (2C2S condition).

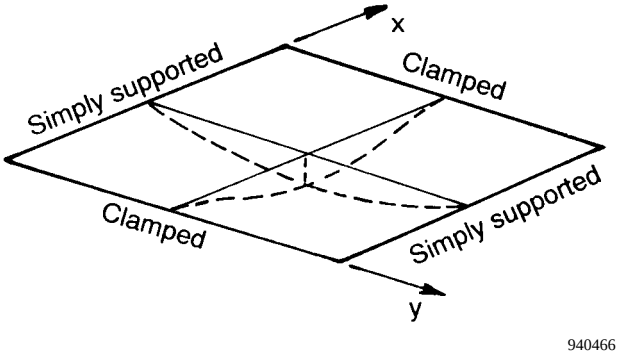

(d) Two sides simply supported, two ends clamped (2S2C condition).

Figure 3. Four types of edge conditions.

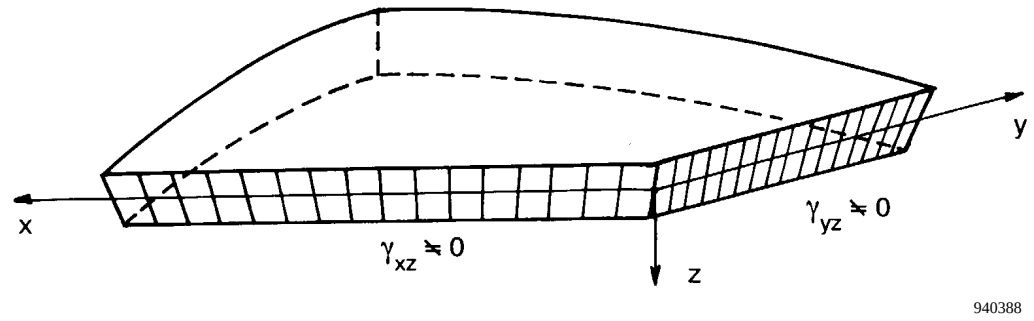

(a) 4S condition.

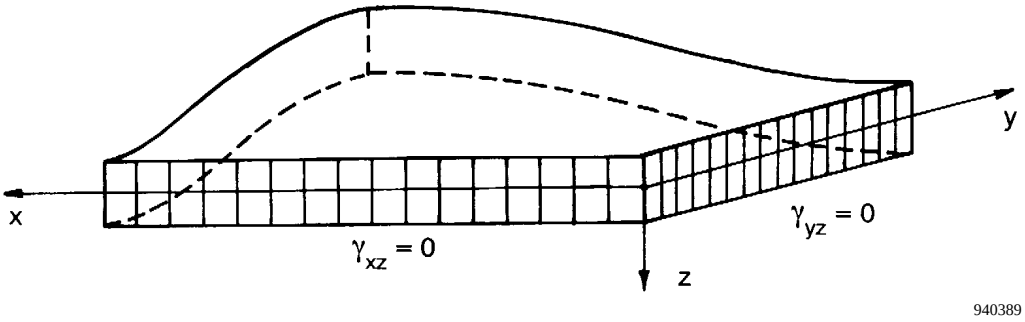

(b) 4C condition.

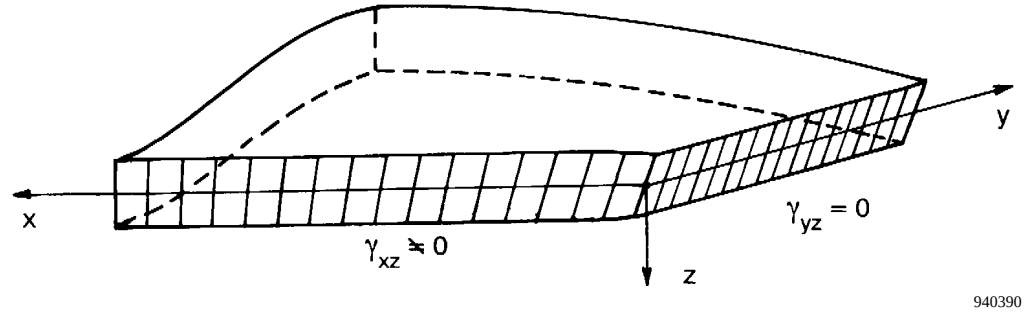

(c) 2C2S condition.

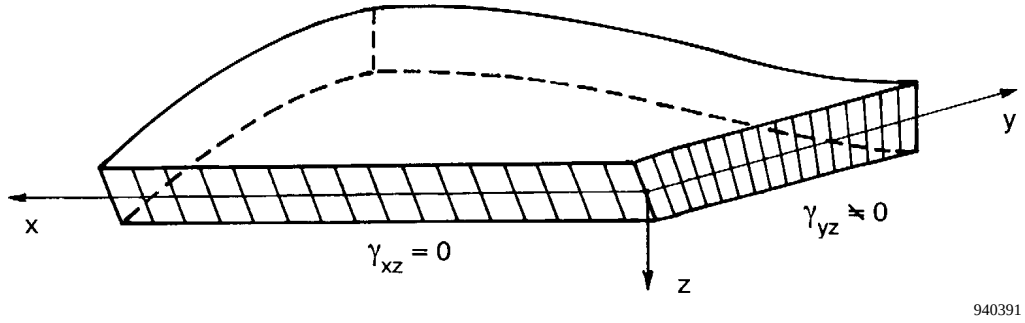

(d) 2S2C condition.

Figure 4. Edge distortions of sandwich panel under different edge conditions; no edge distortions for 4C condition.

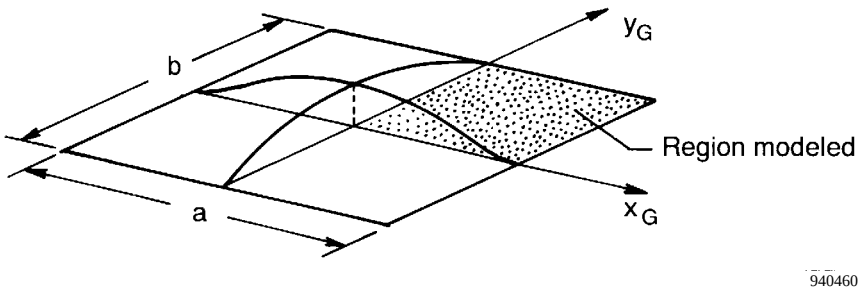

(a) Symmetric buckling (m = 1, n = 1).

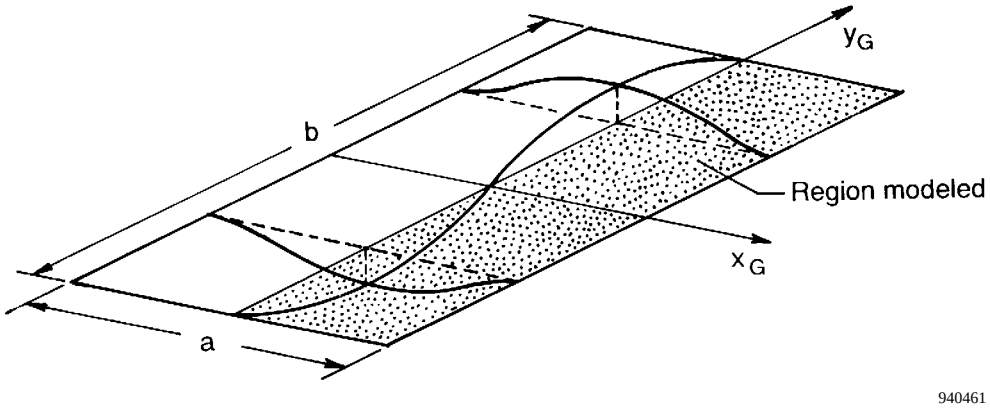

(b) Antisymmetric buckling (m = 1, n = 2).

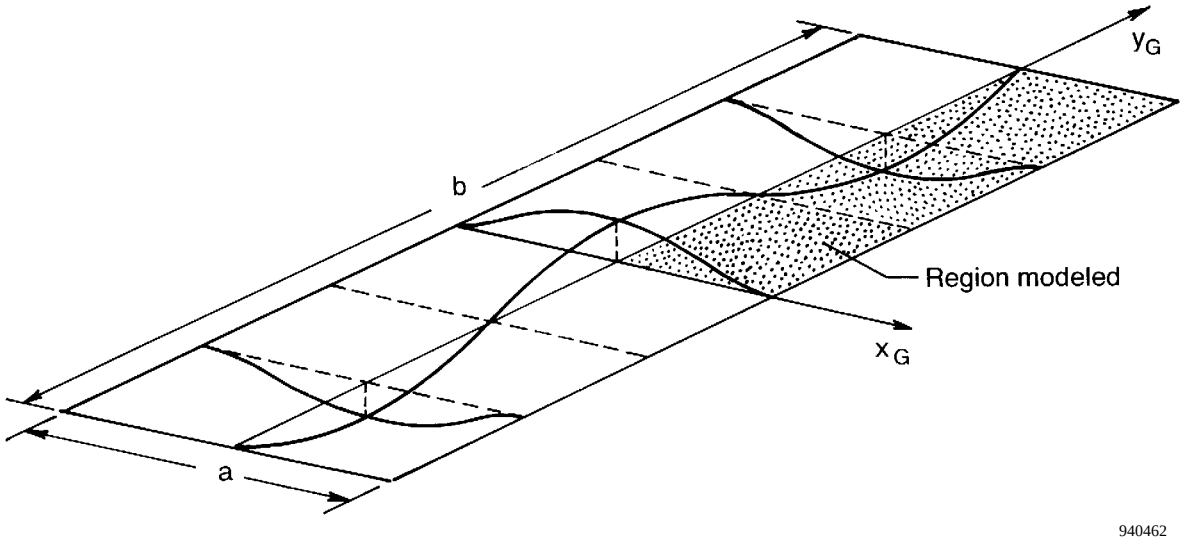

(c) Symmetric buckling (m = 1, n = 3).

Figure 5. Quarter-panel and half-panel regions for finite element models.

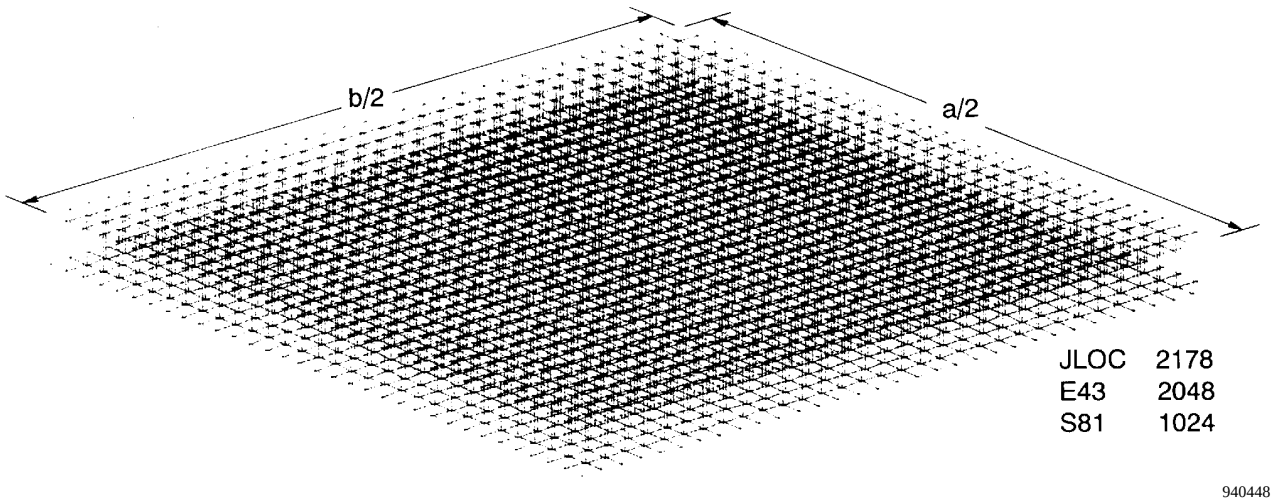

(a) Model A—Quarter-panel model for {m = 1, n = 1}.

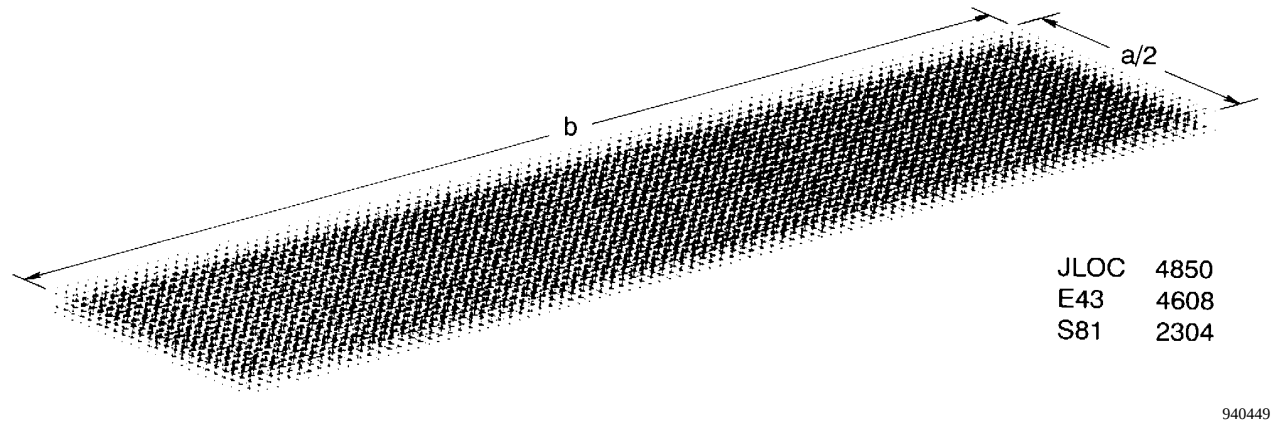

(b) Model B—Half-panel model for {m = 1, n = 2}.

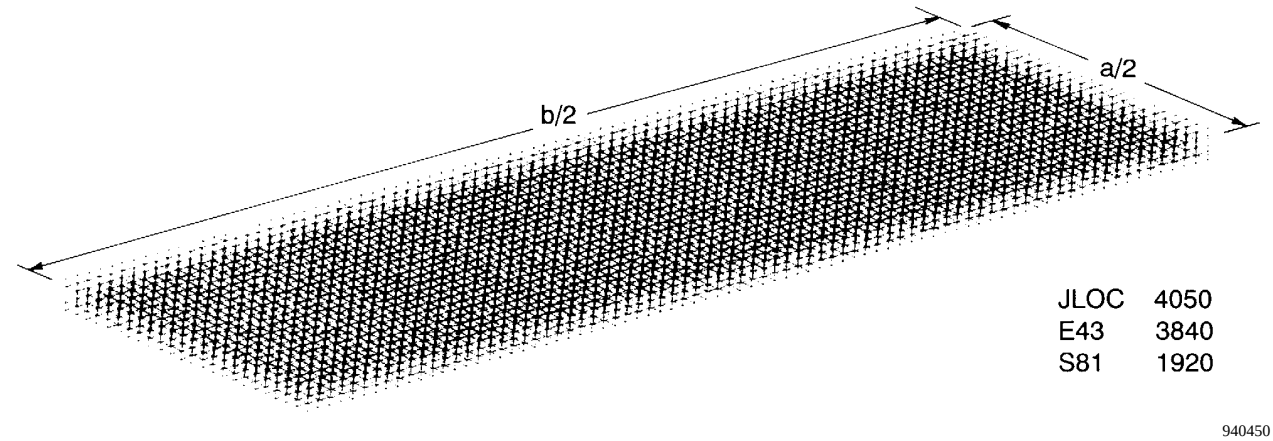

(c) Model C—Quarter-panel model for {m = 1, n = 3}.

Figure 6. Three finite element models generated for sandwich panels of different aspect ratios.

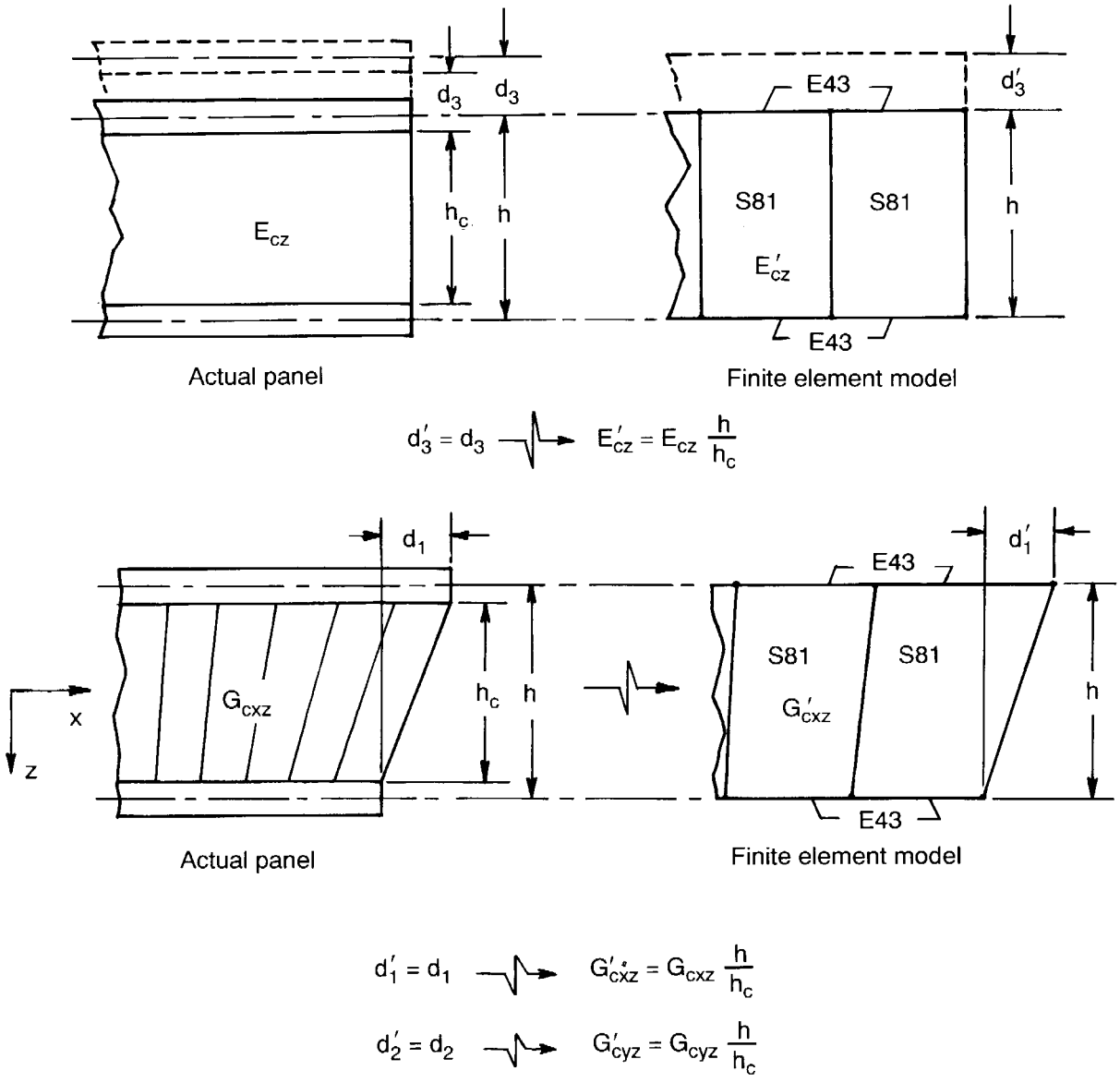

Figure 7. Modeling of sandwich panel.

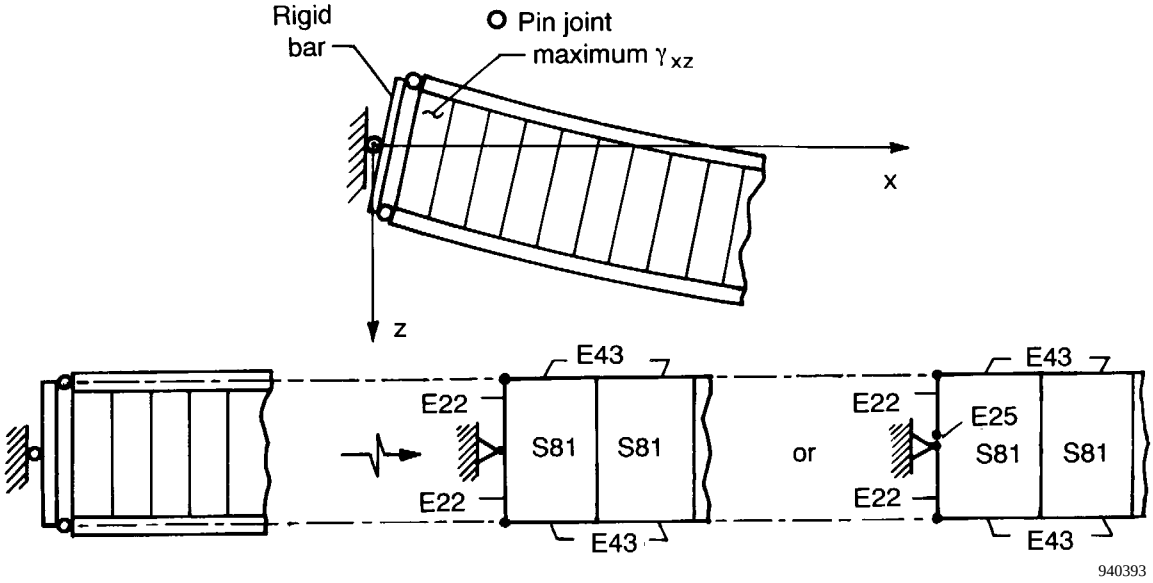

(a) Simply supported edge.

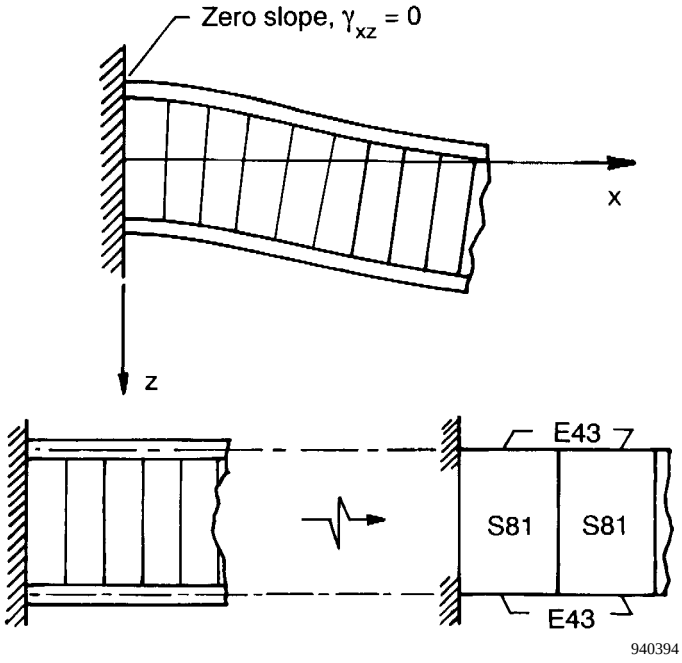

(b) Clamped edge.

Figure 8. Simulation of different edge conditions.

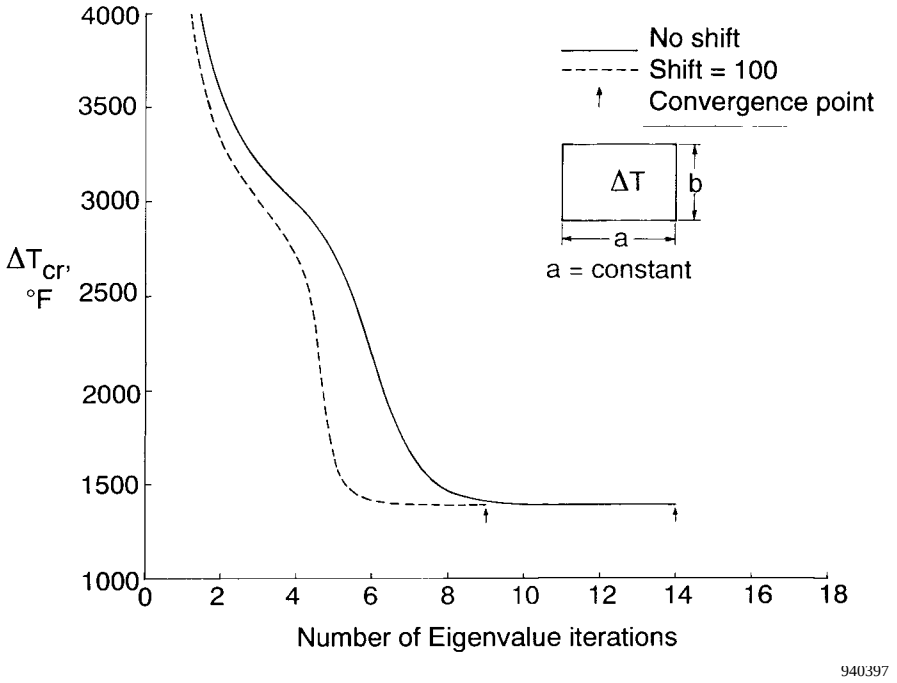

Figure 9. Convergence curves of eigenvalue iterations; 4C condition; *b/a* = 1.

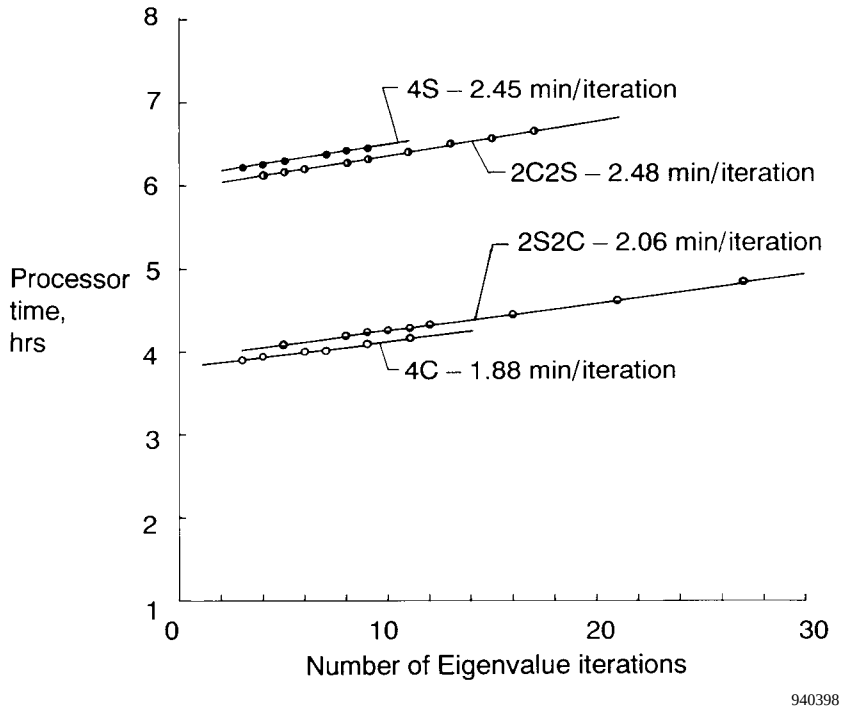

Figure 10. Increase of processor time with number of eigenvalue iterations; ELXSI 6400 computer.

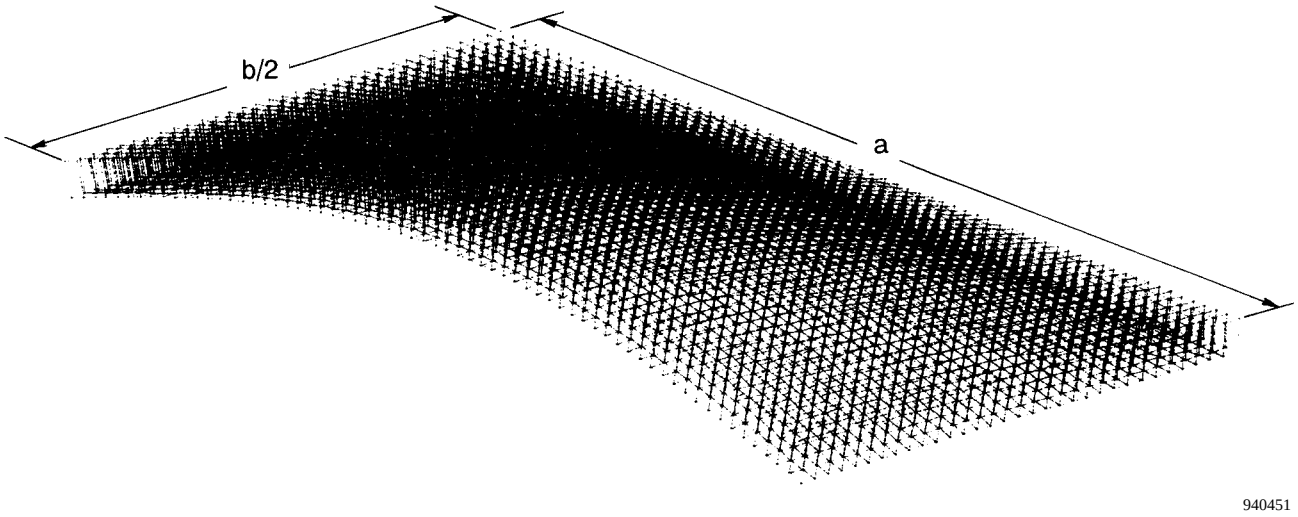

(a) 4S condition {$m = 1$, $n = 1$}.

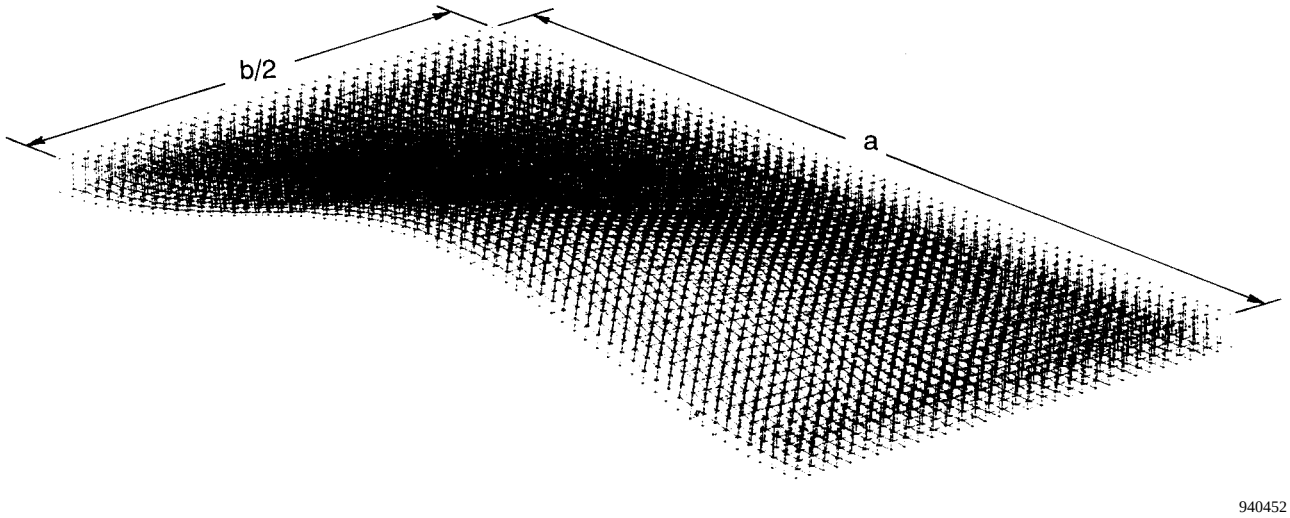

(b) 4C condition {$m = 1$, $n = 1$}.

Figure 11. Buckled shapes of $b/a = 1$ sandwich panel under different edge conditions; half panel.

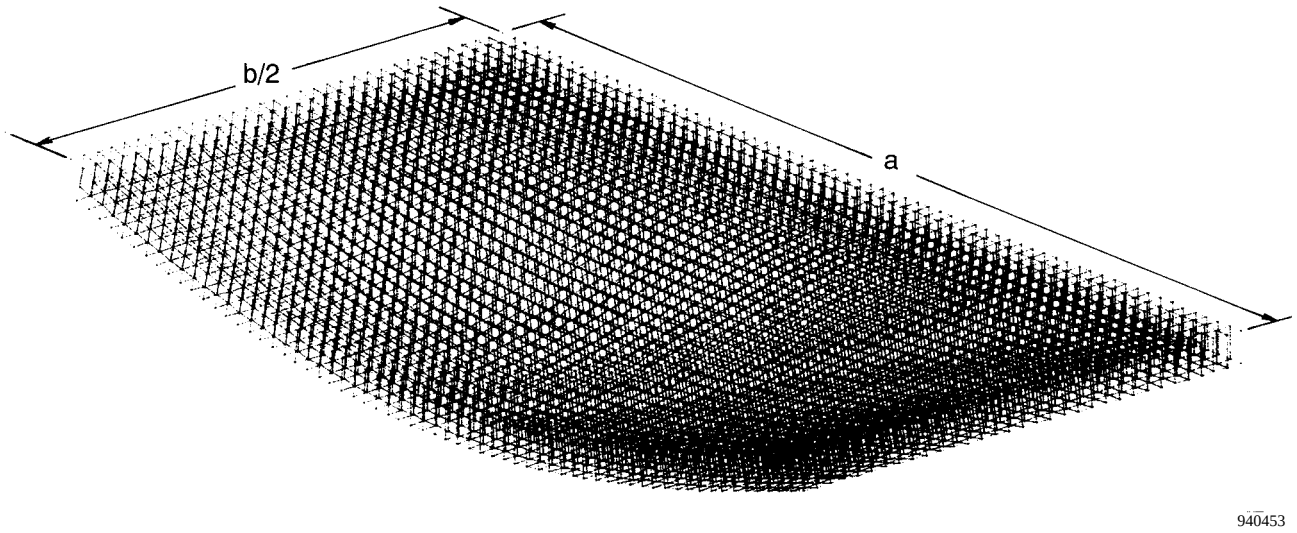

(c) 2C2S condition {$m = 1$, $n = 1$}.

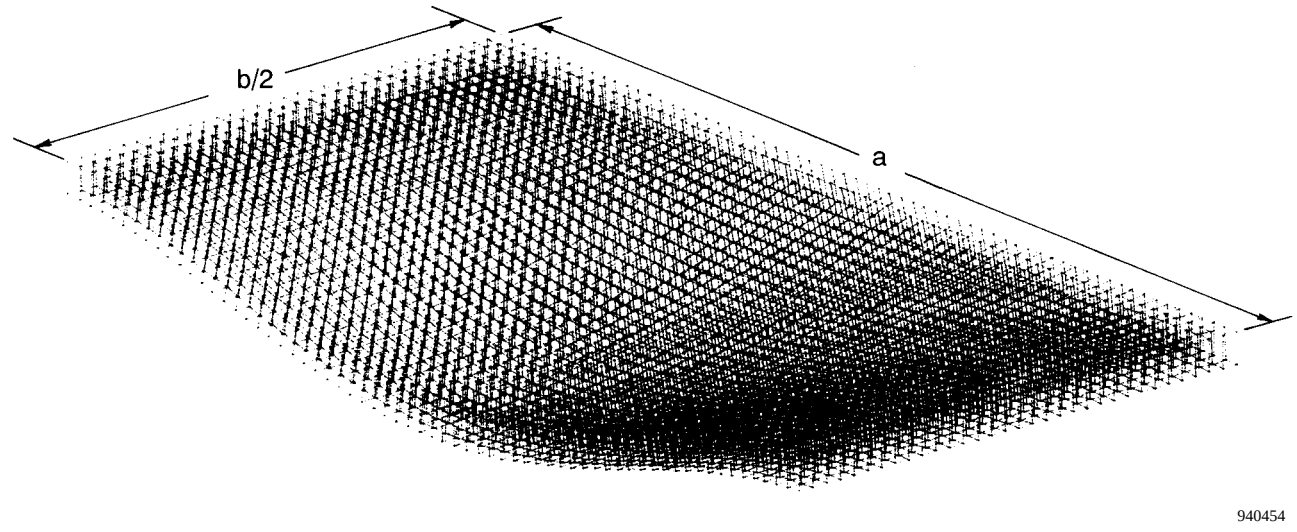

(d) 2S2C condition {$m = 1$, $n = 1$}.

Figure 11. Concluded.

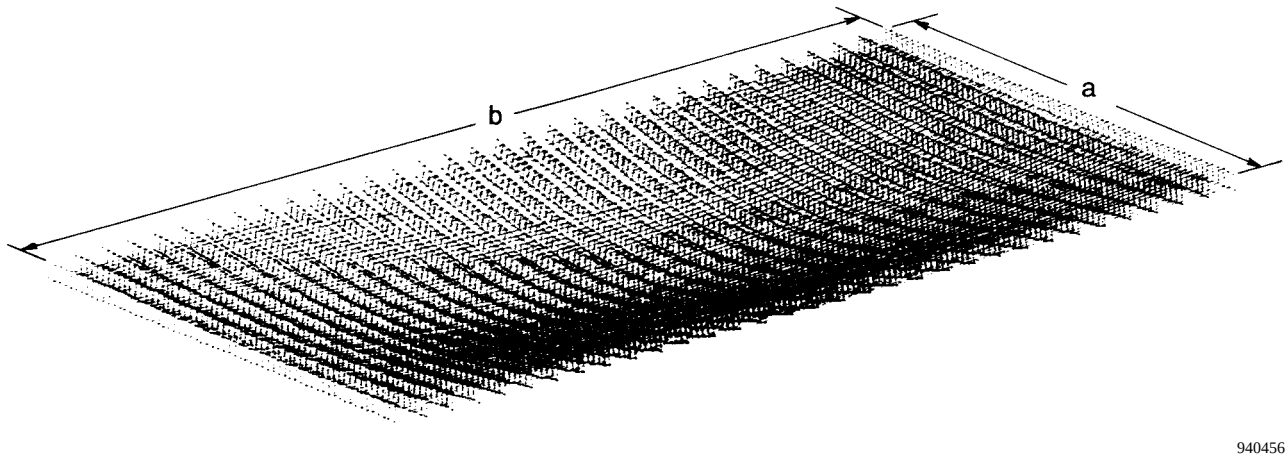

(a) 4S condition {$m = 1$, $n = 1$}.

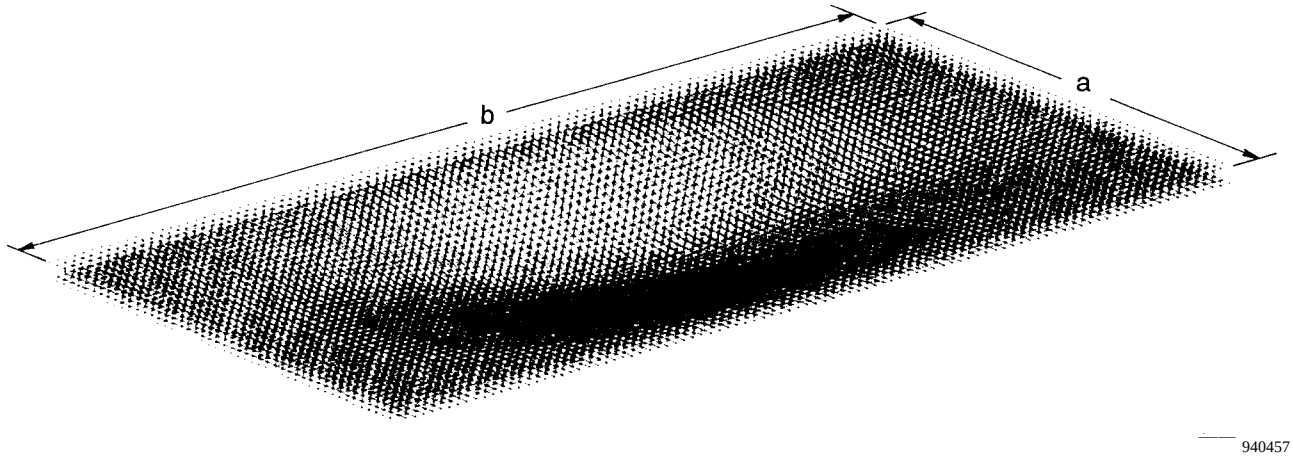

(b) 4C condition {$m = 1$, $n = 1$}.

Figure 12. Buckled shapes of $b/a = 2$ sandwich panel under different edge conditions; full panel.

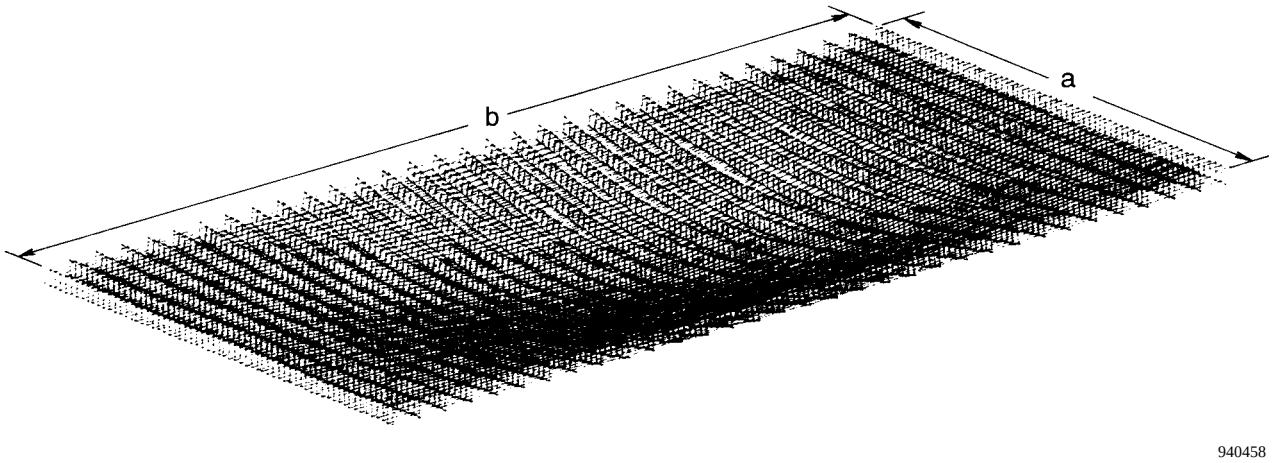

(c) 2C2S condition {$m = 1, n = 1$}.

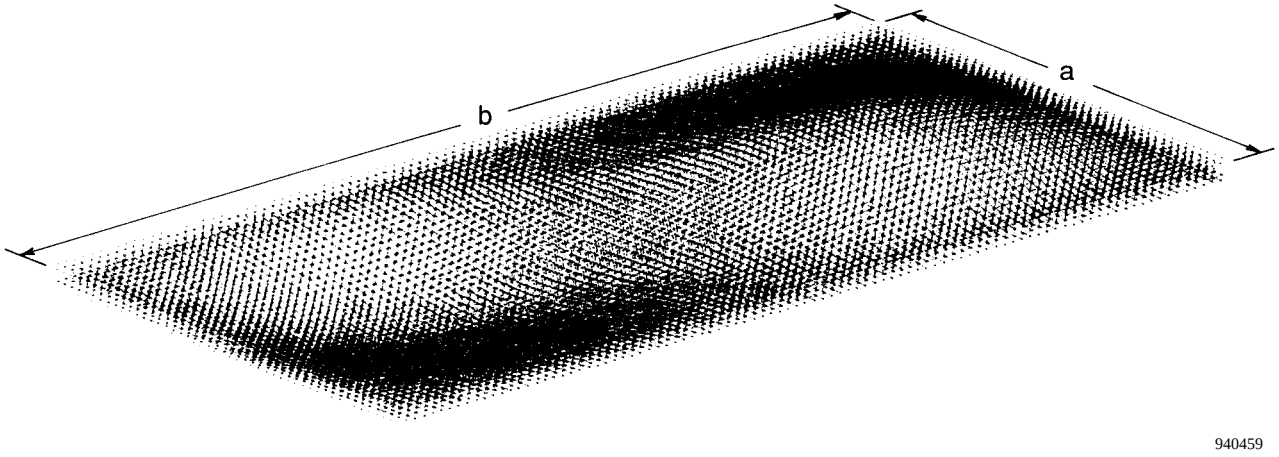

(d) 2S2C condition {$m = 1, n = 2$}.

Figure 12. Concluded.

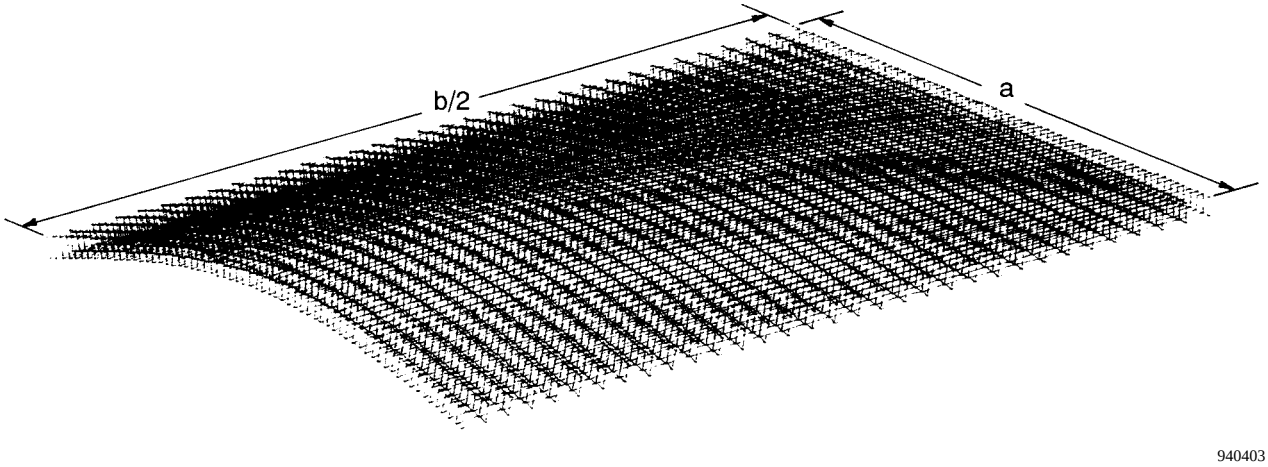

(a) 4S condition {$m = 1$, $n = 1$}.

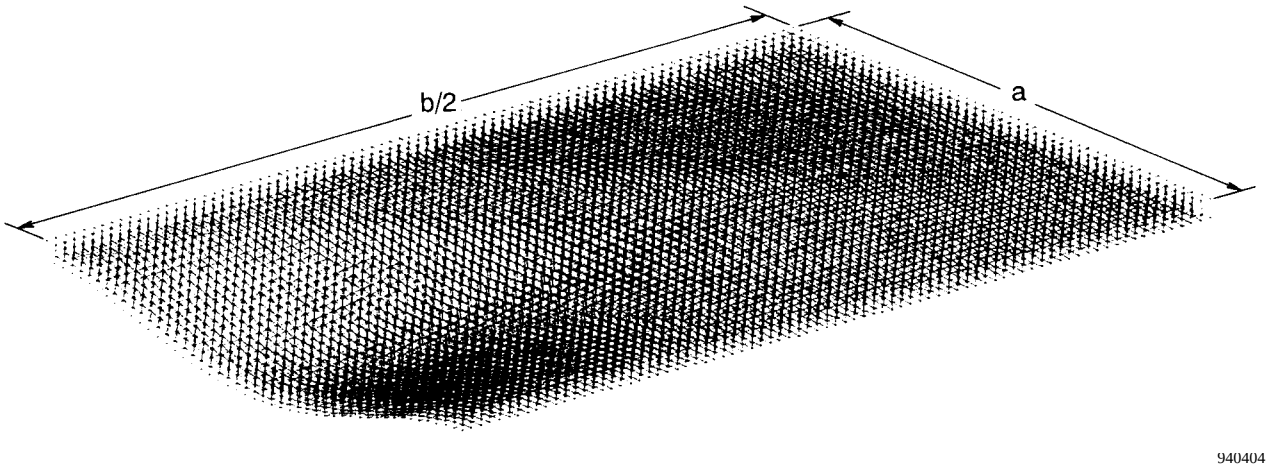

(b) 4C condition {$m = 1$, $n = 3$}.

Figure 13. Buckled shapes of $b/a = 3$ sandwich panel under different edge conditions; half panel.

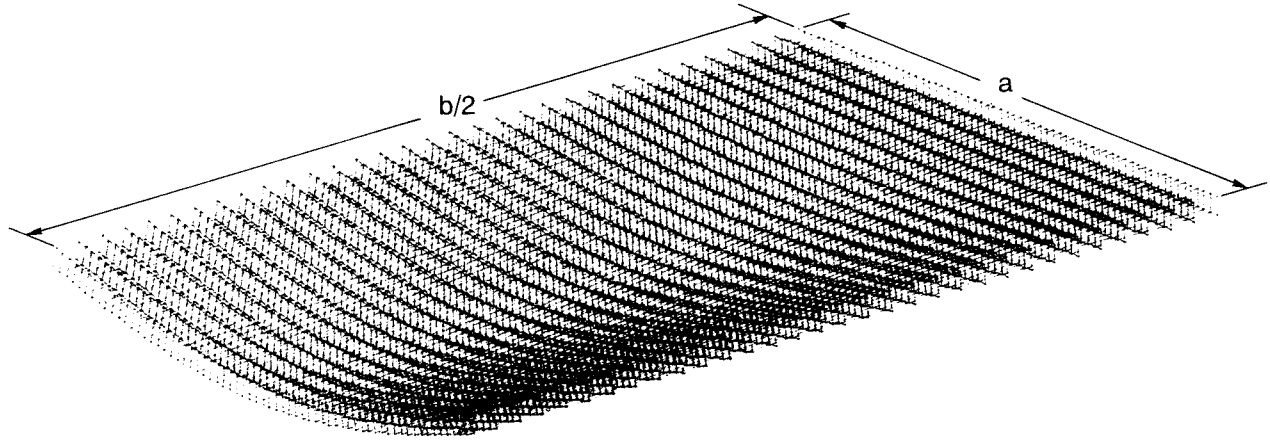

(c) 2C2S condition {$m = 1$, $n = 1$}.

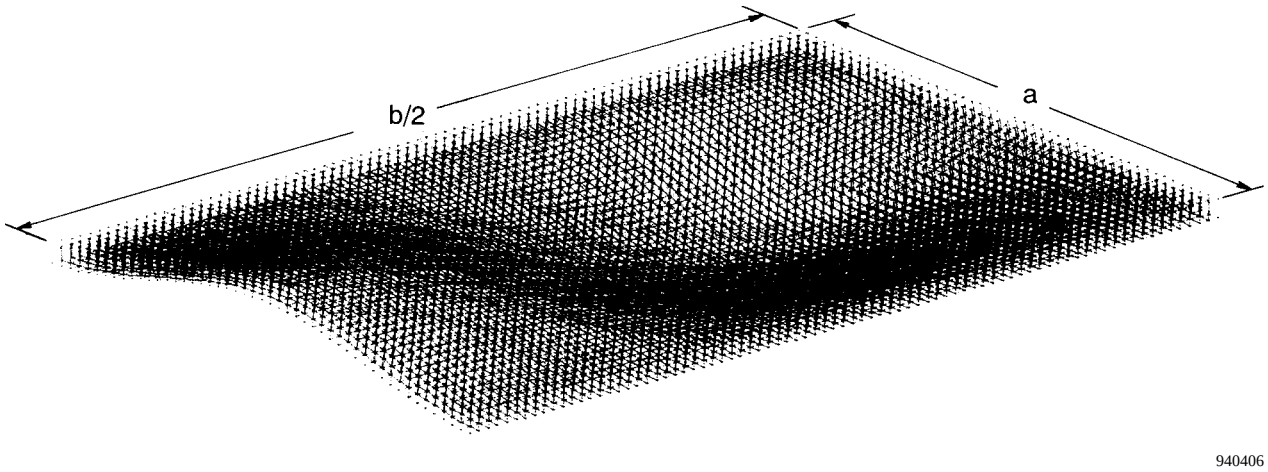

(d) 2S2C condition {$m = 1$, $n = 3$}.

Figure 13. Concluded.

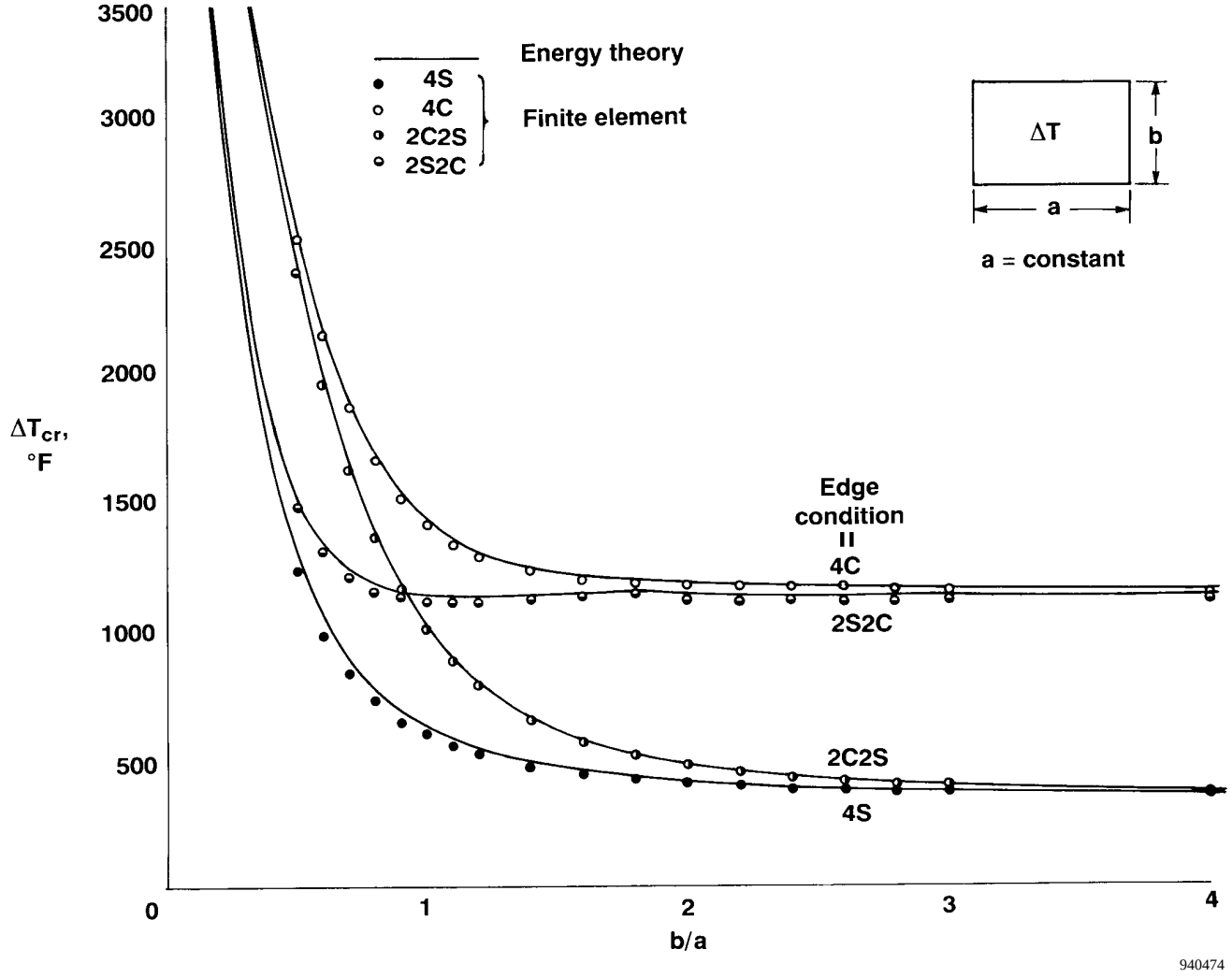

Figure 14. Buckling temperature curves for titanium sandwich panels under different edge conditions; *a* = constant.

APPENDIX A

COEFFICIENTS OF CHARACTERISTIC EQUATIONS

The characteristic coefficients a_{mnkl}^{ij} appearing in equation (22) are defined in the following for different indicial and edge conditions (ref. 12).

Case 1: 4S condition

(1) $\underline{m = k,\ n = l}$

$$
\begin{aligned}
a_{mnmn}^{11} &= D_{11}\left(\frac{m\pi}{a}\right)^4 + 2(D_{12} + 2D_{66})\left(\frac{m\pi}{a}\right)^2\left(\frac{n\pi}{b}\right)^2 + D_{22}\left(\frac{n\pi}{b}\right)^4 \\
&\quad - D^*\left(\frac{\pi}{a}\right)^2\left[k_x\left(\frac{m\pi}{a}\right)^2 + k_y\left(\frac{n\pi}{b}\right)^2\right] \\
a_{mnmn}^{12} &= a_{mnmn}^{21} = -\left[D_{11}\left(\frac{m\pi}{a}\right)^3 + (D_{12} + 2D_{66})\left(\frac{m\pi}{a}\right)\left(\frac{n\pi}{b}\right)^2\right] \\
a_{mnmn}^{13} &= a_{mnmn}^{31} = -\left[D_{22}\left(\frac{n\pi}{b}\right)^3 + (D_{12} + 2D_{66})\left(\frac{m\pi}{a}\right)^2\left(\frac{n\pi}{b}\right)\right] \\
a_{mnmn}^{22} &= D_{11}\left(\frac{m\pi}{a}\right)^2 + D_{66}\left(\frac{n\pi}{b}\right)^2 + D_{Qx} \\
a_{mnmn}^{23} &= a_{mnmn}^{32} = (D_{12} + D_{66})\left(\frac{m\pi}{a}\right)\left(\frac{n\pi}{b}\right) \\
a_{mnmn}^{33} &= D_{22}\left(\frac{n\pi}{b}\right)^2 + D_{66}\left(\frac{m\pi}{a}\right)^2 + D_{Qy}
\end{aligned}
\tag{A-1}
$$

(2) $\underline{m \neq k,\ n \neq l}$

$$
a_{mnkl}^{ij} = 0 \tag{A-2}
$$

Case 2: 4C condition

(1) $\underline{m = n = k = l = 1}$

$$
\begin{aligned}
a_{1111}^{11} &= 12D_{11}\left(\frac{\pi}{a}\right)^4 + 8(D_{12} + 2D_{66})\left(\frac{\pi}{a}\right)^2\left(\frac{\pi}{b}\right)^2 + 12D_{22}\left(\frac{\pi}{b}\right)^4 \\
&\quad - 3D^*\left(\frac{\pi}{a}\right)^2\left[k_x\left(\frac{\pi}{a}\right)^2 + k_y\left(\frac{\pi}{b}\right)^2\right] \\
a_{1111}^{12} &= a_{1111}^{21} = -\left[12D_{11}\left(\frac{\pi}{a}\right)^3 + 4(D_{12} + 2D_{66})\left(\frac{\pi}{a}\right)\left(\frac{\pi}{b}\right)^2\right] \\
a_{1111}^{13} &= a_{1111}^{31} = -\left[12D_{22}\left(\frac{\pi}{b}\right)^3 + 4(D_{12} + 2D_{66})\left(\frac{\pi}{a}\right)^2\left(\frac{\pi}{b}\right)\right] \\
a_{1111}^{22} &= 12D_{11}\left(\frac{\pi}{a}\right)^2 + 4D_{66}\left(\frac{\pi}{b}\right)^2 + 3D_{Qx} \\
a_{1111}^{23} &= a_{1111}^{32} = 4(D_{12} + D_{66})\left(\frac{\pi}{a}\right)\left(\frac{\pi}{b}\right) \\
a_{1111}^{33} &= 12D_{22}\left(\frac{\pi}{b}\right)^2 + 4D_{66}\left(\frac{\pi}{a}\right)^2 + 3D_{Qy}
\end{aligned}
\tag{A-3}
$$

(2) $\underline{m = k = 1,\ n = l \neq 1}$

$$
\begin{aligned}
a_{1n1n}^{11} &= 8D_{11}\left(\frac{\pi}{a}\right)^4 + 4(D_{12} + 2D_{66})\left(\frac{\pi}{a}\right)^2\left(\frac{\pi}{b}\right)^2(1 + n^2) + \frac{3}{2}D_{22}\left(\frac{\pi}{b}\right)^4[(1 + n^2)^2 + 4n^2] \\
&\quad - D^*\left(\frac{\pi}{a}\right)^2\left[2k_x\left(\frac{\pi}{a}\right)^2 + \frac{3}{2}k_y\left(\frac{\pi}{b}\right)^2(1 + n^2)\right] \\
a_{1n1n}^{12} &= a_{1n1n}^{21} = -\left[8D_{11}\left(\frac{\pi}{a}\right)^3 + 2(D_{12} + 2D_{66})\left(\frac{\pi}{a}\right)\left(\frac{\pi}{b}\right)^2(1 + n^2)\right] \\
a_{1n1n}^{13} &= a_{1n1n}^{31} = -\left\{\frac{3}{2}D_{22}\left(\frac{\pi}{b}\right)^3[(1 + n^2)^2 + 4n^2] + 2(D_{12} + 2D_{66})\left(\frac{\pi}{a}\right)^2\left(\frac{\pi}{b}\right)(1 + n^2)\right\} \\
a_{1n1n}^{22} &= 8D_{11}\left(\frac{\pi}{a}\right)^2 + 2D_{66}\left(\frac{\pi}{b}\right)^2(1 + n^2) + 2D_{Qx} \\
a_{1n1n}^{23} &= a_{1n1n}^{32} = 2(D_{12} + D_{66})\left(\frac{\pi}{a}\right)\left(\frac{\pi}{b}\right)(1 + n^2) \\
a_{1n1n}^{33} &= \frac{3}{2}D_{22}\left(\frac{\pi}{b}\right)^2[(1 + n^2)^2 + 4n^2] + 2D_{66}\left(\frac{\pi}{a}\right)^2(1 + n^2) + \frac{3}{2}D_{Qy}(1 + n^2)
\end{aligned}
\tag{A-4}
$$

(3) $\underline{m = k \neq 1, n = l = 1}$

$$
\begin{aligned}
a^{11}_{m1m1} &= \frac{3}{2}D_{11}\left(\frac{\pi}{a}\right)^4[(1+m^2)^2+4m^2]+4(D_{12}+2D_{66})\left(\frac{\pi}{a}\right)^2\left(\frac{\pi}{b}\right)^2(1+m^2)+8D_{22}\left(\frac{\pi}{b}\right)^4 \\
&\quad -D^*\left(\frac{\pi}{a}\right)^2\left[\frac{3}{2}k_x\left(\frac{\pi}{a}\right)^2(1+m^2)+2k_y\left(\frac{\pi}{b}\right)^2\right] \\
a^{12}_{m1m1} &= a^{21}_{m1m1} = -\left\{\frac{3}{2}D_{11}\left(\frac{\pi}{a}\right)^3[(1+m^2)^2+4m^2]+2(D_{12}+2D_{66})\left(\frac{\pi}{a}\right)\left(\frac{\pi}{b}\right)^2(1+m^2)\right\} \\
a^{13}_{m1m1} &= a^{31}_{m1m1} = -\left[8D_{22}\left(\frac{\pi}{b}\right)^3+2(D_{12}+2D_{66})\left(\frac{\pi}{a}\right)^2\left(\frac{\pi}{b}\right)(1+m^2)\right] \\
a^{22}_{m1m1} &= \frac{3}{2}D_{11}\left(\frac{\pi}{a}\right)^2[(1+m^2)^2+4m^2]+2D_{66}\left(\frac{\pi}{b}\right)^2(1+m^2)+\frac{3}{2}D_{Qx}(1+m^2) \\
a^{23}_{m1m1} &= a^{32}_{m1m1} = 2(D_{12}+D_{66})\left(\frac{\pi}{a}\right)\left(\frac{\pi}{b}\right)(1+m^2) \\
a^{33}_{m1m1} &= 8D_{22}\left(\frac{\pi}{b}\right)^2+2D_{66}\left(\frac{\pi}{a}\right)^2(1+m^2)+2D_{Qy}
\end{aligned}
\qquad \text{(A-5)}
$$

(4) $\underline{m = k \neq 1, n = l \neq 1}$

$$
\begin{aligned}
a^{11}_{mnmn} &= D_{11}\left(\frac{\pi}{a}\right)^4[(1+m^2)^2+4m^2]+2(D_{12}+2D_{66})\left(\frac{\pi}{a}\right)^2\left(\frac{\pi}{b}\right)^2(1+m^2)(1+n^2) \\
&\quad +D_{22}\left(\frac{\pi}{b}\right)^4[(1+n^2)^2+4n^2]-D^*\left(\frac{\pi}{a}\right)^2\left[k_x\left(\frac{\pi}{a}\right)^2(1+m^2)+k_y\left(\frac{\pi}{b}\right)^2(1+n^2)\right] \\
a^{12}_{mnmn} &= a^{21}_{mnmn} = -\left\{D_{11}\left(\frac{\pi}{a}\right)^3[(1+m^2)^2+4m^2]+(D_{12}+2D_{66})\left(\frac{\pi}{a}\right)\left(\frac{\pi}{b}\right)^2(1+m^2)(1+n^2)\right\} \\
a^{13}_{mnmn} &= a^{31}_{mnmn} = -\left\{D_{22}\left(\frac{\pi}{b}\right)^3[(1+n^2)^2+4n^2]+(D_{12}+2D_{66})\left(\frac{\pi}{a}\right)^2\left(\frac{\pi}{b}\right)(1+m^2)(1+n^2)\right\} \\
a^{22}_{mnmn} &= D_{11}\left(\frac{\pi}{a}\right)^2[(1+m^2)^2+4m^2]+D_{66}\left(\frac{\pi}{b}\right)^2(1+m^2)(1+n^2)+D_{Qx}(1+m^2) \\
a^{23}_{mnmn} &= a^{32}_{mnmn} = (D_{12}+D_{66})\left(\frac{\pi}{a}\right)\left(\frac{\pi}{b}\right)(1+m^2)(1+n^2) \\
a^{33}_{mnmn} &= D_{22}\left(\frac{\pi}{b}\right)^2[(1+n^2)^2+4n^2]+2D_{66}\left(\frac{\pi}{a}\right)^2(1+m^2)(1+n^2)+D_{Qy}(1+n^2)
\end{aligned}
\qquad \text{(A-6)}
$$

(5) $\underline{m = k = 1,\ n - l = 2}$

$$
\begin{aligned}
a_{1n1l}^{11} &= -\left[4D_{11}\left(\frac{\pi}{a}\right)^4 + 2(D_{12}+2D_{66})\left(\frac{\pi}{a}\right)^2\left(\frac{\pi}{b}\right)^2(1+l)^2 + \frac{3}{4}D_{22}\left(\frac{\pi}{b}\right)^4(1+l)^4\right] \\
&\quad + D^*\left(\frac{\pi}{a}\right)^2\left[k_x\left(\frac{\pi}{a}\right)^2 + \frac{3}{4}k_y\left(\frac{\pi}{b}\right)^2(1+l)^2\right] \\
a_{1n1l}^{12} &= a_{1n1l}^{21} = 4D_{11}\left(\frac{\pi}{a}\right)^3 + (D_{12}+2D_{66})\left(\frac{\pi}{a}\right)\left(\frac{\pi}{b}\right)^2(1+l)^2 \\
a_{1n1l}^{13} &= a_{1n1l}^{31} = \frac{3}{4}D_{22}\left(\frac{\pi}{b}\right)^3(1+l)^4 + (D_{12}+2D_{66})\left(\frac{\pi}{a}\right)^2\left(\frac{\pi}{b}\right)(1+l)^2 \\
a_{1n1l}^{22} &= -\left[4D_{11}\left(\frac{\pi}{a}\right)^2 + D_{66}\left(\frac{\pi}{b}\right)^2(1+l)^2 + D_{Qx}\right] \\
a_{1n1l}^{23} &= a_{1n1l}^{32} = -(D_{12}+D_{66})\left(\frac{\pi}{a}\right)\left(\frac{\pi}{b}\right)(1+l)^2 \\
a_{1n1l}^{33} &= -\left[\frac{3}{4}D_{22}\left(\frac{\pi}{b}\right)^2(1+l)^4 + D_{66}\left(\frac{\pi}{a}\right)^2(1+l)^2 + \frac{3}{4}D_{Qy}(1+l)^2\right]
\end{aligned}
\tag{A-7}
$$

(6) $\underline{m = k \neq 1,\ n - l = 2}$

$$
\begin{aligned}
a_{mnml}^{11} &= -\frac{1}{2}\left\{D_{11}\left(\frac{\pi}{4}\right)^4[(1+m^2)^2 + 4m^2] + 2(D_{12}+2D_{66})\left(\frac{\pi}{a}\right)^2\left(\frac{\pi}{b}\right)^2(1+m^2)(1+l)^2\right. \\
&\quad \left. + D_{22}\left(\frac{\pi}{b}\right)^4(1+l)^4\right\} + \frac{D^*}{2}\left(\frac{\pi}{a}\right)^2\left[k_x\left(\frac{\pi}{a}\right)^2(1+m^2) + k_y\left(\frac{\pi}{b}\right)^2(1+l)^2\right] \\
a_{mnml}^{12} &= a_{mnml}^{21} = \frac{1}{2}\left\{D_{11}\left(\frac{\pi}{a}\right)^3[(1+m^2)^2 + 4m^2] + (D_{12}+2D_{66})\left(\frac{\pi}{a}\right)\left(\frac{\pi}{b}\right)^2(1+m^2)(1+l)^2\right\} \\
a_{mnml}^{13} &= a_{mnml}^{31} = \frac{1}{2}\left\{D_{22}\left(\frac{\pi}{b}\right)^3(1+l)^4 + (D_{12}+2D_{66})\left(\frac{\pi}{a}\right)^2\left(\frac{\pi}{b}\right)(1+m^2)(1+l)^2\right\} \\
a_{mnml}^{22} &= -\frac{1}{2}\left\{D_{11}\left(\frac{\pi}{a}\right)^2[(1+m^2)^2 + 4m^2] + D_{66}\left(\frac{\pi}{b}\right)^2(1+m^2)(1+l)^2 + D_{Qx}(1+m^2)\right\} \\
a_{mnml}^{23} &= a_{mnml}^{32} = -\frac{1}{2}(D_{12}+D_{66})\left(\frac{\pi}{a}\right)\left(\frac{\pi}{b}\right)(1+m^2)(1+l)^2 \\
a_{mnml}^{33} &= -\frac{1}{2}\left[D_{22}\left(\frac{\pi}{b}\right)^2(1+l)^4 + D_{66}\left(\frac{\pi}{a}\right)^2(1+m^2)(1+l)^2 + D_{Qy}(1+l)^2\right]
\end{aligned}
\tag{A-8}
$$

(7) $\underline{m-k=2,\ n=l=1}$

$$
\begin{aligned}
a^{11}_{m1k1} &= -\left[\frac{3}{4}D_{11}\left(\frac{\pi}{a}\right)^4(1+k)^4 + 2(D_{12}+2D_{66})\left(\frac{\pi}{a}\right)^2\left(\frac{\pi}{b}\right)^2(1+k)^2 + 4D_{22}\left(\frac{\pi}{b}\right)^4\right] \\
&\quad + D^*\left(\frac{\pi}{a}\right)^2\left[\frac{3}{4}k_x\left(\frac{\pi}{a}\right)^2(1+k)^2 + k_y\left(\frac{\pi}{b}\right)^2\right] \\
a^{12}_{m1k1} &= a^{21}_{mlkl} = \frac{3}{4}D_{11}\left(\frac{\pi}{a}\right)^3(1+k)^4 + (D_{12}+2D_{66})\left(\frac{\pi}{a}\right)\left(\frac{\pi}{b}\right)^2(1+k)^2 \\
a^{13}_{m1k1} &= a^{31}_{mlkl} = 4D_{22}\left(\frac{\pi}{b}\right)^3 + (D_{12}+2D_{66})\left(\frac{\pi}{a}\right)^2\left(\frac{\pi}{b}\right)(1+k)^2 \\
a^{22}_{m1k1} &= -\left[\frac{3}{4}D_{11}\left(\frac{\pi}{a}\right)^2(1+k)^4 + D_{66}\left(\frac{\pi}{b}\right)^2(1+k)^2 + \frac{3}{4}D_{Qx}(1+k)^2\right] \\
a^{23}_{m1k1} &= a^{32}_{mlkl} = -(D_{12}+D_{66})\left(\frac{\pi}{a}\right)\left(\frac{\pi}{b}\right)(1+k)^2 \\
a^{33}_{m1k1} &= -\left[4D_{22}\left(\frac{\pi}{b}\right)^2 + D_{66}\left(\frac{\pi}{a}\right)^2(1+k)^2 + D_{Qy}\right]
\end{aligned}
\tag{A-9}
$$

(8) $\underline{m-k=2,\ n=l\neq 1}$

$$
\begin{aligned}
a^{11}_{mnkn} &= -\frac{1}{2}\left\{D_{11}\left(\frac{\pi}{a}\right)^4(1+k)^4 + 2(D_{12}+2D_{66})\left(\frac{\pi}{a}\right)^2\left(\frac{\pi}{b}\right)^2(1+k)^2(1+n^2)\right. \\
&\quad \left. + D_{22}\left(\frac{\pi}{b}\right)^4[(1+n^2)^2+4n^2]\right\} + \frac{D^*}{2}\left(\frac{\pi}{a}\right)^2\left[k_x\left(\frac{\pi}{a}\right)^2(1+k)^2 + k_y\left(\frac{\pi}{b}\right)^2(1+n^2)\right] \\
a^{12}_{mnkn} &= a^{21}_{mnkn} = \frac{1}{2}\left[D_{11}\left(\frac{\pi}{a}\right)^3(1+k)^4 + (D_{12}+2D_{66})\left(\frac{\pi}{a}\right)\left(\frac{\pi}{b}\right)^2(1+k)^2(1+n^2)\right] \\
a^{13}_{mnkn} &= a^{31}_{mnkn} = \frac{1}{2}\left[D_{22}\left(\frac{\pi}{b}\right)^3[(1+n^2)^2+4n^2] + (D_{12}+2D_{66})\left(\frac{\pi}{a}\right)^2\left(\frac{\pi}{b}\right)(1+k)^2(1+n^2)\right] \\
a^{22}_{mnkn} &= -\frac{1}{2}\left[D_{11}\left(\frac{\pi}{a}\right)^2(1+k)^4 + D_{66}\left(\frac{\pi}{b}\right)^2(1+k)^2(1+n^2) + D_{Qx}(1+k)^2\right] \\
a^{23}_{mnkn} &= a^{32}_{mnkn} = -\frac{1}{2}(D_{12}+D_{66})\left(\frac{\pi}{a}\right)\left(\frac{\pi}{b}\right)(1+k)^2(1+n^2) \\
a^{33}_{mnkn} &= -\frac{1}{2}\left\{D_{22}\left(\frac{\pi}{b}\right)^2[(1+n^2)^2+4n^2] + D_{66}\left(\frac{\pi}{a}\right)^2(1+k^2)(1+n^2) + D_{Qy}(1+n^2)\right\}
\end{aligned}
\tag{A-10}
$$

(9) $\underline{m-k=2,\ n-l=2}$

$$
\begin{aligned}
a^{11}_{mnkl} &= \frac{1}{4}\left[D_{11}\left(\frac{\pi}{a}\right)^4(1+k)^4 + 2(D_{12}+2D_{66})\left(\frac{\pi}{a}\right)^2\left(\frac{\pi}{b}\right)^2(1+k)^2(1+l)^2\right. \\
&\quad \left. + D_{22}\left(\frac{\pi}{b}\right)^4(1+l)^4\right] - \frac{D^*}{4}\left(\frac{\pi}{a}\right)^2\left[k_x\left(\frac{\pi}{a}\right)^2(1+k)^2 + k_y\left(\frac{\pi}{b}\right)^2(1+l)^2\right] \\
a^{12}_{mnkl} &= a^{21}_{mnkl} = -\frac{1}{4}\left[D_{11}\left(\frac{\pi}{a}\right)^3(1+k)^4 + (D_{12}+2D_{66})\left(\frac{\pi}{a}\right)\left(\frac{\pi}{b}\right)^2(1+k)^2(1+l)^2\right] \\
a^{13}_{mnkl} &= a^{31}_{mnkl} = -\frac{1}{4}\left[D_{22}\left(\frac{\pi}{b}\right)^3(1+l)^4 + (D_{12}+2D_{66})\left(\frac{\pi}{a}\right)^2\left(\frac{\pi}{b}\right)(1+k)^2(1+l)^2\right] \\
a^{22}_{mnkl} &= \frac{1}{4}\left[D_{11}\left(\frac{\pi}{a}\right)^2(1+k)^4 + D_{66}\left(\frac{\pi}{b}\right)^2(1+k)^2(1+l)^2 + D_{Qx}(1+k)^2\right] \\
a^{23}_{mnkl} &= a^{32}_{mnkl} = \frac{1}{4}(D_{12}+D_{66})\left(\frac{\pi}{a}\right)\left(\frac{\pi}{b}\right)(1+k)^2(1+l)^2 \\
a^{33}_{mnkl} &= \frac{1}{4}\left[D_{22}\left(\frac{\pi}{b}\right)^2(1+l)^4 + D_{66}\left(\frac{\pi}{a}\right)^2(1+k)^2(1+l)^2 + D_{Qy}(1+l)^2\right]
\end{aligned}
\qquad \text{(A-11)}
$$

Case 3: 2C2S condition

(1) $\underline{m=k,\ n=l=1}$

$$
\begin{aligned}
a^{11}_{m1m1} &= 3D_{11}\left(\frac{m\pi}{a}\right)^4 + 8(D_{12}+2D_{66})\left(\frac{m\pi}{a}\right)^2\left(\frac{\pi}{b}\right)^2 + 16D_{22}\left(\frac{\pi}{b}\right)^4 \\
&\quad - D^*\left(\frac{\pi}{a}\right)^2\left[3k_x\left(\frac{m\pi}{a}\right)^2 + 4k_y\left(\frac{\pi}{b}\right)^2\right] \\
a^{12}_{m1m1} &= a^{21}_{m1m1} = -\left[3D_{11}\left(\frac{m\pi}{a}\right)^3 + 4(D_{12}+2D_{66})\left(\frac{m\pi}{a}\right)\left(\frac{\pi}{b}\right)^2\right] \\
a^{13}_{m1m1} &= a^{31}_{m1m1} = -\left[16D_{22}\left(\frac{\pi}{b}\right)^3 + 4(D_{12}+2D_{66})\left(\frac{m\pi}{a}\right)^2\left(\frac{\pi}{b}\right)\right] \\
a^{22}_{m1m1} &= 3D_{11}\left(\frac{m\pi}{a}\right)^2 + 4D_{66}\left(\frac{\pi}{b}\right)^2 + 3D_{Qx} \\
a^{23}_{m1m1} &= a^{32}_{m1m1} = 4(D_{12}+D_{66})\left(\frac{m\pi}{a}\right)\left(\frac{\pi}{b}\right) \\
a^{33}_{m1m1} &= 16D_{22}\left(\frac{\pi}{b}\right)^2 + 4D_{66}\left(\frac{m\pi}{a}\right)^2 + 4D_{Qx}
\end{aligned}
\qquad \text{(A-12)}
$$

(2) $\underline{m = k,\ n = l \neq 1}$

$$
\begin{aligned}
a^{11}_{mnmn} &= 2D_{11}\left(\frac{m\pi}{a}\right)^4 + 4(D_{12} + 2D_{66})\left(\frac{m\pi}{a}\right)^2\left(\frac{\pi}{b}\right)^2(1+n^2) + 2D_{22}\left(\frac{\pi}{b}\right)^4[(1+n^2)^2 + 4n^2] \\
&\quad - 2D^*\left(\frac{\pi}{a}\right)^2\left[k_x\left(\frac{m\pi}{a}\right)^2 + k_y\left(\frac{\pi}{b}\right)^2(1+n^2)\right] \\
a^{12}_{mnmn} &= a^{21}_{mnmn} = -\left[2D_{11}\left(\frac{m\pi}{a}\right)^3 + 2(D_{12} + 2D_{66})\left(\frac{m\pi}{a}\right)\left(\frac{\pi}{b}\right)^2(1+n^2)\right] \\
a^{13}_{mnmn} &= a^{31}_{mnmn} = -\left\{2D_{22}\left(\frac{\pi}{b}\right)^3[(1+n^2)^2 + 4n^2] + 2(D_{12} + 2D_{66})\left(\frac{m\pi}{a}\right)^2\left(\frac{\pi}{b}\right)(1+n^2)\right\} \\
a^{22}_{mnmn} &= 2D_{11}\left(\frac{m\pi}{a}\right)^2 + 2D_{66}\left(\frac{\pi}{b}\right)^2(1+n^2) + 2D_{Qx} \\
a^{23}_{mnmn} &= a^{32}_{mnmn} = 2(D_{12} + D_{66})\left(\frac{m\pi}{a}\right)\left(\frac{\pi}{b}\right)(1+n^2) \\
a^{33}_{mnmn} &= 2D_{22}\left(\frac{\pi}{b}\right)^2[(1+n^2)^2 + 4n^2] + 2D_{66}\left(\frac{m\pi}{a}\right)^2(1+n^2) + 2D_{Qy}(1+n^2)
\end{aligned}
\qquad \text{(A-13)}
$$

(3) $\underline{m = k,\ n - l = 2}$

$$
\begin{aligned}
a^{11}_{mnml} &= -\left[D_{11}\left(\frac{m\pi}{a}\right)^4 + 2(D_{12} + 2D_{66})\left(\frac{m\pi}{a}\right)^2\left(\frac{\pi}{b}\right)^2(1+l)^2 + D_{22}\left(\frac{\pi}{b}\right)^4(1+l)^4\right] \\
&\quad + D^*\left(\frac{\pi}{a}\right)^2\left[k_x\left(\frac{m\pi}{a}\right)^2 + k_y\left(\frac{\pi}{b}\right)^2(1+l)^2\right] \\
a^{12}_{mnml} &= a^{21}_{mnml} = D_{11}\left(\frac{m\pi}{a}\right)^3 + (D_{12} + 2D_{66})\left(\frac{m\pi}{a}\right)\left(\frac{\pi}{b}\right)^2(1+l)^2 \\
a^{13}_{mnml} &= a^{31}_{mnml} = D_{22}\left(\frac{\pi}{b}\right)^3(1+l)^4 + (D_{12} + 2D_{66})\left(\frac{m\pi}{a}\right)^2\left(\frac{\pi}{b}\right)(1+l)^2 \\
a^{22}_{mnml} &= -\left[D_{11}\left(\frac{m\pi}{a}\right)^2 + D_{66}\left(\frac{\pi}{b}\right)^2(1+l)^2 + D_{Qx}\right] \\
a^{23}_{mnml} &= a^{32}_{mnml} = -(D_{12} + D_{66})\left(\frac{m\pi}{a}\right)\left(\frac{\pi}{b}\right)(1+l)^2 \\
a^{33}_{mnml} &= -\left[D_{22}\left(\frac{\pi}{b}\right)^2(1+l)^4 + D_{66}\left(\frac{m\pi}{a}\right)^2(1+l)^2 + D_{Qy}(1+l)^2\right]
\end{aligned}
\qquad \text{(A-14)}
$$

Case 4: 2S2C condition

(1) $\underline{m = k = 1,\ n = 1}$

$$
\begin{aligned}
a_{1n1n}^{11} &= 16D_{11}\left(\frac{\pi}{a}\right)^4 + 8(D_{12} + 2D_{66})\left(\frac{\pi}{a}\right)^2\left(\frac{n\pi}{b}\right)^2 + 3D_{22}\left(\frac{n\pi}{b}\right)^4 \\
&\quad - D^*\left(\frac{\pi}{a}\right)^2\left[4k_x\left(\frac{\pi}{a}\right)^2 + 3k_y\left(\frac{n\pi}{b}\right)^2\right] \\
a_{1n1n}^{12} &= a_{1n1n}^{21} = -\left[16D_{11}\left(\frac{\pi}{a}\right)^3 + 4(D_{12} + 2D_{66})\left(\frac{\pi}{a}\right)\left(\frac{n\pi}{b}\right)^2\right] \\
a_{1n1n}^{13} &= a_{1n1n}^{31} = -\left[3D_{22}\left(\frac{n\pi}{b}\right)^3 + 4(D_{12} + 2D_{66})\left(\frac{\pi}{a}\right)^2\left(\frac{n\pi}{b}\right)\right] \\
a_{1n1n}^{22} &= 16D_{11}\left(\frac{\pi}{a}\right)^2 + 4D_{66}\left(\frac{n\pi}{b}\right)^2 + 4D_{Qx} \\
a_{1n1n}^{23} &= a_{1n1n}^{32} = 4(D_{12} + D_{66})\left(\frac{\pi}{a}\right)\left(\frac{n\pi}{b}\right) \\
a_{1n1n}^{33} &= 3D_{22}\left(\frac{n\pi}{b}\right)^2 + 4D_{66}\left(\frac{\pi}{a}\right)^2 + 3D_{Qx}
\end{aligned}
\tag{A-15}
$$

(2) $\underline{m = k \neq 1,\ n = 1}$

$$
\begin{aligned}
a_{mnmn}^{11} &= 2D_{11}\left(\frac{\pi}{a}\right)^4[(1+m^2)^2 + 4m^2] + 4(D_{12} + 2D_{66})\left(\frac{\pi}{a}\right)^2\left(\frac{n\pi}{b}\right)^2(1+m^2) + 2D_{22}\left(\frac{n\pi}{b}\right)^4 \\
&\quad - 2D^*\left(\frac{\pi}{a}\right)^2\left[k_x\left(\frac{\pi}{a}\right)^2(1+m^2) + k_y\left(\frac{n\pi}{b}\right)^2\right] \\
a_{mnmn}^{12} &= a_{mnmn}^{21} = -\left\{2D_{11}\left(\frac{\pi}{a}\right)^3[(1+m^2)^2 + 4m^2] + 2(D_{12} + 2D_{66})\left(\frac{\pi}{a}\right)\left(\frac{n\pi}{b}\right)^2(1+m^2)\right\} \\
a_{mnmn}^{13} &= a_{mnmn}^{31} = -\left[2D_{22}\left(\frac{n\pi}{b}\right)^3 + 2(D_{12} + 2D_{66})(1+m^2)\left(\frac{\pi}{a}\right)^2\left(\frac{n\pi}{b}\right)\right] \\
a_{mnmn}^{22} &= 2D_{11}\left(\frac{\pi}{a}\right)^2[(1+m^2)^2 + 4m^2] + 2D_{66}\left(\frac{n\pi}{b}\right)^2(1+m^2) + 2D_{Qy}(1+m^2) \\
a_{mnmn}^{23} &= a_{mnmn}^{32} = 2(D_{12} + D_{66})\left(\frac{\pi}{a}\right)\left(\frac{n\pi}{b}\right)(1+m^2) \\
a_{mnmn}^{33} &= 2D_{22}\left(\frac{n\pi}{b}\right)^2 + 2D_{66}\left(\frac{\pi}{a}\right)^2(1+m^2) + 2D_{Qy}
\end{aligned}
\tag{A-16}
$$

(3) $\underline{m-k=2,\ n=1}$

$$
\begin{aligned}
a^{11}_{mnkn} &= -\left[D_{11}\left(\frac{\pi}{a}\right)^4(1+k)^4 + 2(D_{12}+2D_{66})\left(\frac{\pi}{a}\right)^2\left(\frac{n\pi}{b}\right)^2(1+k)^2 + D_{22}\left(\frac{n\pi}{b}\right)^4\right] \\
&\quad + D^*\left(\frac{\pi}{a}\right)^2\left[k_x\left(\frac{\pi}{a}\right)^2(1+k)^2 + k_y\left(\frac{n\pi}{b}\right)^2\right] \\
a^{12}_{mnkn} &= a^{21}_{mnkn} = D_{11}\left(\frac{\pi}{a}\right)^3(1+k)^4 + (D_{12}+2D_{66})\left(\frac{\pi}{a}\right)\left(\frac{n\pi}{b}\right)^2(1+k)^2 \\
a^{13}_{mnkn} &= a^{31}_{mnkn} = D_{22}\left(\frac{n\pi}{b}\right)^3 + (D_{12}+2D_{66})\left(\frac{\pi}{a}\right)^2\left(\frac{n\pi}{b}\right)(1+k)^2 \qquad \text{(A-17)} \\
a^{22}_{mnkn} &= -\left[D_{11}\left(\frac{\pi}{a}\right)^2(1+k)^4 + D_{66}\left(\frac{n\pi}{b}\right)^2(1+k)^2 + D_{Qx}(1+k)^2\right] \\
a^{23}_{mnkn} &= a^{32}_{mnkn} = -(D_{12}+D_{66})\left(\frac{\pi}{a}\right)\left(\frac{n\pi}{b}\right)(1+k)^2 \\
a^{33}_{mnkn} &= -\left[D_{22}\left(\frac{n\pi}{b}\right)^2 + D_{66}\left(\frac{\pi}{a}\right)^2(1+k)^2 + D_{Qy}\right]
\end{aligned}
$$

APPENDIX B

BUCKLING EQUATIONS

The buckling equations (eigenvalue solution equations) written out from equation (21) up to order 12 (i.e., 12×12 matrices) for the cases $m \pm n$ = even (symmetric buckling) and $m \pm n$ = odd (antisymmetric buckling) for different edge conditions are given on the following pages (ref. 12).

Case 1: 4S condition
$m \pm n$ = even (symmetric buckling)

$A_{kl} \rightarrow$	A_{11}	A_{13}	A_{22}	A_{31}	A_{15}	A_{24}	A_{33}	A_{42}	A_{51}	A_{35}	A_{44}	A_{53}
m=1, n=1	$\frac{M_{1111}}{\Delta T} + P_{1111}$	0	$\frac{4}{9}$	0	0	$\frac{8}{45}$	0	$\frac{8}{45}$	0	0	$\frac{16}{225}$	0
m=1, n=3		$\frac{M_{1313}}{\Delta T} + P_{1313}$	$-\frac{4}{5}$	0	0	$\frac{8}{7}$	0	$-\frac{8}{25}$	0	0	$\frac{16}{35}$	0
m=2, n=2			$\frac{M_{2222}}{\Delta T} + P_{2222}$	$-\frac{4}{5}$	$-\frac{20}{63}$	0	$\frac{36}{25}$	0	$-\frac{20}{63}$	$\frac{4}{7}$	0	$\frac{4}{7}$
m=3, n=1				$\frac{M_{3131}}{\Delta T} + P_{3131}$	0	$-\frac{8}{25}$	0	$\frac{8}{7}$	0	0	$\frac{16}{35}$	0
m=1, n=5					$\frac{M_{1515}}{\Delta T} + P_{1515}$	$-\frac{40}{27}$	0	$-\frac{8}{63}$	0	0	$-\frac{16}{27}$	0
m=2, n=4						$\frac{M_{2424}}{\Delta T} + P_{2424}$	$-\frac{72}{35}$	0	$-\frac{8}{63}$	$\frac{8}{3}$	0	$-\frac{120}{147}$
m=3, n=3							$\frac{M_{3333}}{\Delta T} + P_{3333}$	$-\frac{72}{35}$	0	0	$\frac{144}{49}$	0
m=4, n=2			Symmetry					$\frac{M_{4242}}{\Delta T} + P_{4242}$	$-\frac{40}{27}$	$-\frac{120}{147}$	0	$\frac{8}{3}$
m=5, n=1									$\frac{M_{5151}}{\Delta T} + P_{5151}$	0	$-\frac{16}{27}$	0
m=3, n=5										$\frac{M_{3535}}{\Delta T} + P_{3535}$	$-\frac{80}{21}$	0
m=4, n=4											$\frac{M_{4444}}{\Delta T} + P_{4444}$	$-\frac{80}{21}$
m=5, n=3												$\frac{M_{5353}}{\Delta T} + P_{5353}$

$= 0$

(B-1)

$m \pm n$ = odd (antisymmetric buckling) (4S)

$$
\begin{array}{l|cccccccccccc|l}
A_{kl} \rightarrow & A_{12} & A_{21} & A_{14} & A_{23} & A_{32} & A_{41} & A_{16} & A_{25} & A_{34} & A_{43} & A_{52} & A_{61} & \\
\hline
m{=}1,\ n{=}2 & \frac{M_{1212}}{\Delta T} + P_{1212} & -\frac{4}{9} & 0 & \frac{4}{5} & 0 & -\frac{8}{45} & 0 & \frac{20}{63} & 0 & \frac{8}{25} & 0 & -\frac{4}{35} & \\
m{=}2,\ n{=}1 & & \frac{M_{2121}}{\Delta T} + P_{2121} & -\frac{8}{45} & 0 & \frac{4}{5} & 0 & -\frac{4}{35} & 0 & \frac{8}{25} & 0 & \frac{20}{63} & 0 & \\
m{=}1,\ n{=}4 & & & \frac{M_{1414}}{\Delta T} + P_{1414} & -\frac{8}{7} & 0 & -\frac{16}{225} & 0 & \frac{40}{27} & 0 & -\frac{16}{35} & 0 & -\frac{8}{175} & \\
m{=}2,\ n{=}3 & & & & \frac{M_{2323}}{\Delta T} + P_{2323} & -\frac{36}{25} & 0 & -\frac{4}{9} & 0 & \frac{72}{35} & 0 & -\frac{4}{7} & 0 & \\
m{=}3,\ n{=}2 & & & & & \frac{M_{3232}}{\Delta T} + P_{3232} & -\frac{8}{7} & 0 & -\frac{4}{7} & 0 & \frac{72}{35} & 0 & -\frac{4}{9} & \\
m{=}4,\ n{=}1 & & & & & & \frac{M_{4141}}{\Delta T} + P_{4141} & -\frac{8}{175} & 0 & -\frac{16}{35} & 0 & \frac{40}{27} & 0 & = 0 \\
m{=}1,\ n{=}6 & & & & & & & \frac{M_{1616}}{\Delta T} + P_{1616} & -\frac{20}{11} & 0 & -\frac{8}{45} & 0 & -\frac{36}{1225} & \\
m{=}2,\ n{=}5 & & & \text{Symmetry} & & & & & \frac{M_{2525}}{\Delta T} + P_{2525} & -\frac{8}{3} & 0 & -\frac{100}{441} & 0 & \\
m{=}3,\ n{=}4 & & & & & & & & & \frac{M_{3434}}{\Delta T} + P_{3434} & -\frac{144}{49} & 0 & -\frac{8}{45} & \\
m{=}4,\ n{=}3 & & & & & & & & & & \frac{M_{4343}}{\Delta T} + P_{4343} & -\frac{8}{3} & 0 & \\
m{=}5,\ n{=}2 & & & & & & & & & & & \frac{M_{5252}}{\Delta T} + P_{5252} & -\frac{20}{11} & \\
m{=}6,\ n{=}1 & & & & & & & & & & & & \frac{M_{6161}}{\Delta T} + P_{6161} &
\end{array}
$$

(B-2)

Case 2: 4C condition
$m \pm n$ = even (symmetric buckling)

$A_{kl} \rightarrow$	A_{11}	A_{13}	A_{22}	A_{31}	A_{15}	A_{24}	A_{33}	A_{42}	A_{51}	A_{35}	A_{44}	A_{53}
m=1, n=1	$\frac{M_{1111}}{\Delta T} + P_{1111}$	$\frac{M_{1113}}{\Delta T} + P_{1113}$	$\frac{4}{225}$	$\frac{M_{1131}}{\Delta T} + P_{1131}$	0	$-\frac{8}{1575}$	$\frac{M_{1133}}{\Delta T} + P_{1133}$	$-\frac{8}{1575}$	0	0	$\frac{16}{11025}$	0
m=1, n=3		$\frac{M_{1313}}{\Delta T} + P_{1313}$	$-\frac{44}{1575}$	$\frac{M_{1331}}{\Delta T} + P_{1331}$	$\frac{M_{1315}}{\Delta T} + P_{1315}$	$\frac{184}{4725}$	$\frac{M_{1333}}{\Delta T} + P_{1333}$	$\frac{88}{11025}$	0	$\frac{M_{1335}}{\Delta T} + P_{1335}$	$-\frac{368}{33075}$	0
m=2, n=2			$\frac{M_{2222}}{\Delta T} + P_{2222}$	$-\frac{44}{1575}$	$\frac{4}{525}$	$\frac{M_{2224}}{\Delta T} + P_{2224}$	$\frac{484}{11025}$	$\frac{M_{2242}}{\Delta T} + P_{2242}$	$\frac{4}{525}$	$-\frac{44}{3675}$	$\frac{M_{2244}}{\Delta T} + P_{2244}$	$-\frac{44}{3675}$
m=3, n=1				$\frac{M_{3131}}{\Delta T} + P_{3131}$	0	$\frac{88}{11025}$	$\frac{M_{3133}}{\Delta T} + P_{3133}$	$\frac{184}{4725}$	$\frac{M_{3151}}{\Delta T} + P_{3151}$	0	$-\frac{368}{33075}$	$\frac{M_{3153}}{\Delta T} + P_{3153}$
m=1, n=5					$\frac{M_{1515}}{\Delta T} + P_{1515}$	$-\frac{104}{2079}$	$\frac{M_{1533}}{\Delta T} + P_{1533}$	$-\frac{8}{3675}$	0	$\frac{M_{1535}}{\Delta T} + P_{1535}$	$\frac{208}{14553}$	0
m=2, n=4						$\frac{M_{2424}}{\Delta T} + P_{2424}$	$-\frac{2024}{33075}$	$\frac{M_{2442}}{\Delta T} + P_{2442}$	$-\frac{8}{3675}$	$\frac{104}{1323}$	$\frac{M_{2444}}{\Delta T} + P_{2444}$	$\frac{184}{11025}$
m=3, n=3							$\frac{M_{3333}}{\Delta T} + P_{3333}$	$-\frac{2024}{33075}$	$\frac{M_{3351}}{\Delta T} + P_{3351}$	$\frac{M_{3335}}{\Delta T} + P_{3335}$	$\frac{8464}{99225}$	$\frac{M_{3353}}{\Delta T} + P_{3353}$
m=4, n=2			Symmetry					$\frac{M_{4242}}{\Delta T} + P_{4242}$	$-\frac{104}{2079}$	$\frac{184}{11025}$	$\frac{M_{4244}}{\Delta T} + P_{4244}$	$\frac{104}{1323}$
m=5, n=1									$\frac{M_{5151}}{\Delta T} + P_{5151}$	0	$\frac{208}{14553}$	$\frac{M_{5153}}{\Delta T} + P_{5153}$
m=3, n=5										$\frac{M_{3535}}{\Delta T} + P_{3535}$	$-\frac{4784}{43659}$	$\frac{M_{3553}}{\Delta T} + P_{3553}$
m=4, n=4											$\frac{M_{4444}}{\Delta T} + P_{4444}$	$-\frac{4784}{43659}$
m=5, n=3												$\frac{M_{5353}}{\Delta T} + P_{5353}$

$= 0$ (B-3)

$m \pm n$ = odd (antisymmetric buckling) (4C)

$A_{kl} \rightarrow$	A_{12}	A_{21}	A_{14}	A_{23}	A_{32}	A_{41}	A_{16}	A_{25}	A_{34}	A_{43}	A_{52}	A_{61}
m=1, n=2	$\frac{M_{1212}}{\Delta T} + P_{1212}$	$-\frac{4}{225}$	$\frac{M_{1214}}{\Delta T} + P_{1214}$	$\frac{44}{1575}$	$\frac{M_{1232}}{\Delta T} + P_{1232}$	$\frac{8}{1575}$	0	$-\frac{4}{525}$	$\frac{M_{1234}}{\Delta T} + P_{1234}$	$-\frac{88}{11025}$	0	$\frac{4}{4725}$
m=2, n=1		$\frac{M_{2121}}{\Delta T} + P_{2121}$	$\frac{8}{1575}$	$\frac{M_{2123}}{\Delta T} + P_{2123}$	$\frac{44}{1575}$	$\frac{M_{2141}}{\Delta T} + P_{2141}$	$\frac{4}{4725}$	0	$-\frac{88}{11025}$	$\frac{M_{2143}}{\Delta T} + P_{2143}$	$-\frac{4}{525}$	0
m=1, n=4			$\frac{M_{1414}}{\Delta T} + P_{1414}$	$-\frac{184}{4725}$	$\frac{M_{1432}}{\Delta T} + P_{1432}$	$-\frac{16}{11025}$	$\frac{M_{1416}}{\Delta T} + P_{1416}$	$\frac{104}{2079}$	$\frac{M_{1434}}{\Delta T} + P_{1434}$	$\frac{368}{33075}$	0	$-\frac{8}{33075}$
m=2, n=3				$\frac{M_{2323}}{\Delta T} + P_{2323}$	$-\frac{484}{11025}$	$\frac{M_{2341}}{\Delta T} + P_{2341}$	$\frac{172}{17325}$	$\frac{M_{2325}}{\Delta T} + P_{2325}$	$\frac{2024}{33075}$	$\frac{M_{2343}}{\Delta T} + P_{2343}$	$\frac{44}{3675}$	0
m=3, n=2					$\frac{M_{3232}}{\Delta T} + P_{3232}$	$-\frac{184}{4725}$	0	$\frac{44}{3675}$	$\frac{M_{3234}}{\Delta T} + P_{3234}$	$\frac{2024}{33075}$	$\frac{M_{3252}}{\Delta T} + P_{3252}$	$\frac{172}{17325}$
m=4, n=1						$\frac{M_{4141}}{\Delta T} + P_{4141}$	$-\frac{8}{33075}$	0	$\frac{368}{33075}$	$\frac{M_{4143}}{\Delta T} + P_{4143}$	$\frac{104}{2079}$	$\frac{M_{4161}}{\Delta T} + P_{4161}$
m=1, n=6							$\frac{M_{1616}}{\Delta T} + P_{1616}$	$-\frac{236}{3861}$	$\frac{M_{1634}}{\Delta T} + P_{1634}$	$-\frac{344}{121275}$	0	$-\frac{4}{99225}$
m=2, n=5			Symmetry					$\frac{M_{2525}}{\Delta T} + P_{2525}$	$-\frac{104}{1323}$	$\frac{M_{2543}}{\Delta T} + P_{2543}$	$-\frac{4}{1225}$	0
m=3, n=4									$\frac{M_{3434}}{\Delta T} + P_{3434}$	$-\frac{8464}{99225}$	$\frac{M_{3452}}{\Delta T} + P_{3452}$	$-\frac{344}{121275}$
m=4, n=3										$\frac{M_{4343}}{\Delta T} + P_{4343}$	$-\frac{104}{1323}$	$\frac{M_{4361}}{\Delta T} + P_{4361}$
m=5, n=2											$\frac{M_{5252}}{\Delta T} + P_{5252}$	$-\frac{236}{3861}$
m=6, n=1												$\frac{M_{6161}}{\Delta T} + P_{6161}$

$= 0$

(B-4)

Case 3: 2C2S condition
$m \pm n$ = even (symmetric buckling)

$A_{kl} \rightarrow$	A_{11}	A_{13}	A_{22}	A_{31}	A_{15}	A_{24}	A_{33}	A_{42}	A_{51}	A_{35}	A_{44}	A_{53}
m=1, n=1	$\frac{M_{1111}}{\Delta T} + P_{1111}$	$\frac{M_{1113}}{\Delta T} + P_{1113}$	$\frac{4}{45}$	0	0	$-\frac{8}{315}$	0	$\frac{8}{225}$	0	0	$-\frac{16}{1575}$	0
m=1, n=3		$\frac{M_{1313}}{\Delta T} + P_{1313}$	$-\frac{44}{315}$	0	$\frac{M_{1315}}{\Delta T} + P_{1315}$	$\frac{184}{945}$	0	$-\frac{88}{1575}$	0	0	$\frac{368}{4725}$	0
m=2, n=2			$\frac{M_{2222}}{\Delta T} + P_{2222}$	$-\frac{4}{25}$	$\frac{4}{105}$	$\frac{M_{2224}}{\Delta T} + P_{2224}$	$\frac{44}{175}$	0	$-\frac{4}{63}$	$-\frac{12}{175}$	0	$\frac{44}{441}$
m=3, n=1				$\frac{M_{3131}}{\Delta T} + P_{3131}$	0	$\frac{8}{175}$	$\frac{M_{3133}}{\Delta T} + P_{3133}$	$\frac{8}{35}$	0	0	$-\frac{16}{245}$	0
m=1, n=5					$\frac{M_{1515}}{\Delta T} + P_{1515}$	$-\frac{520}{2079}$	0	$\frac{8}{525}$	0	0	$-\frac{208}{2079}$	0
m=2, n=4						$\frac{M_{2424}}{\Delta T} + P_{2424}$	$-\frac{184}{525}$	0	$\frac{8}{441}$	$\frac{104}{231}$	0	$-\frac{184}{1323}$
m=3, n=3							$\frac{M_{3333}}{\Delta T} + P_{3333}$	$-\frac{88}{245}$	0	$\frac{M_{3335}}{\Delta T} + P_{3335}$	$\frac{368}{735}$	0
m=4, n=2			Symmetry					$\frac{M_{4242}}{\Delta T} + P_{4242}$	$-\frac{8}{27}$	$\frac{24}{245}$	$\frac{M_{4244}}{\Delta T} + P_{4244}$	$\frac{88}{189}$
m=5, n=1									$\frac{M_{5151}}{\Delta T} + P_{5151}$	0	$\frac{16}{189}$	$\frac{M_{5153}}{\Delta T} + P_{5153}$
m=3, n=5										$\frac{M_{3535}}{\Delta T} + P_{3535}$	$-\frac{1040}{1617}$	0
m=4, n=4											$\frac{M_{4444}}{\Delta T} + P_{4444}$	$-\frac{368}{567}$
m=5, n=3												$\frac{M_{5353}}{\Delta T} + P_{5353}$

$= 0$

(B-5)

$m \pm n$ = odd (antisymmetric buckling) (2C2S)

$A_{kl} \rightarrow$	A_{12}	A_{21}	A_{14}	A_{23}	A_{32}	A_{41}	A_{16}	A_{25}	A_{34}	A_{43}	A_{52}	A_{61}	
m=1, n=2	$\frac{M_{1212}}{\Delta T} + P_{1212}$	$-\frac{4}{25}$	$\frac{M_{1214}}{\Delta T} + P_{1214}$	$\frac{44}{315}$	0	$-\frac{8}{225}$	0	$-\frac{4}{105}$	0	$\frac{88}{1575}$	0	$-\frac{4}{175}$	
m=2, n=1		$\frac{M_{2121}}{\Delta T} + P_{2121}$	$\frac{8}{315}$	$\frac{M_{2123}}{\Delta T} + P_{2123}$	$\frac{4}{25}$	0	$\frac{4}{925}$	0	$-\frac{8}{175}$	0	$\frac{4}{63}$	0	
m=1, n=4			$\frac{M_{1414}}{\Delta T} + P_{1414}$	$-\frac{184}{945}$	0	$\frac{16}{1575}$	$\frac{M_{1416}}{\Delta T} + P_{1416}$	$\frac{520}{2079}$	0	$-\frac{368}{4725}$	0	$\frac{8}{1225}$	
m=2, n=3				$\frac{M_{2323}}{\Delta T} + P_{2323}$	$-\frac{44}{175}$	0	$\frac{172}{3465}$	$\frac{M_{2325}}{\Delta T} + P_{2325}$	$\frac{184}{525}$	0	$-\frac{44}{441}$	0	
m=3, n=2					$\frac{M_{3232}}{\Delta T} + P_{3232}$	$-\frac{8}{35}$	0	$\frac{12}{175}$	$\frac{M_{3234}}{\Delta T} + P_{3234}$	$\frac{88}{245}$	0	$-\frac{4}{45}$	
m=4, n=1						$\frac{M_{4141}}{\Delta T} + P_{4141}$	$\frac{8}{4725}$	0	$\frac{16}{245}$	$\frac{M_{4143}}{\Delta T} + P_{4143}$	$\frac{8}{27}$	0	$= 0$
m=1, n=6							$\frac{M_{1616}}{\Delta T} + P_{1616}$	$-\frac{1180}{3861}$	0	$\frac{344}{17325}$	0	$\frac{4}{3675}$	
m=2, n=5			Symmetry					$\frac{M_{2525}}{\Delta T} + P_{2525}$	$-\frac{104}{231}$	0	$\frac{4}{147}$	0	
m=3, n=4									$\frac{M_{3434}}{\Delta T} + P_{3434}$	$-\frac{368}{735}$	0	$\frac{8}{315}$	
m=4, n=3										$\frac{M_{4343}}{\Delta T} + P_{4343}$	$-\frac{88}{189}$	0	
m=5, n=2											$\frac{M_{5252}}{\Delta T} + P_{5252}$	$-\frac{4}{11}$	
m=6, n=1												$\frac{M_{6161}}{\Delta T} + P_{6161}$	

(B-6)

Case 4: 2S2C condition
$m \pm n$ = even (symmetric buckling)

$A_{kl} \rightarrow$	A_{11}	A_{13}	A_{22}	A_{31}	A_{15}	A_{24}	A_{33}	A_{42}	A_{51}	A_{35}	A_{44}	A_{53}
m=1, n=1	$\frac{M_{1111}}{\Delta T} + P_{1111}$	0	$\frac{4}{45}$	$\frac{M_{1131}}{\Delta T} + P_{1131}$	0	$\frac{8}{225}$	0	$-\frac{8}{315}$	0	0	$-\frac{16}{1575}$	0
m=1, n=3		$\frac{M_{1313}}{\Delta T} + P_{1313}$	$-\frac{4}{25}$	0	0	$\frac{8}{35}$	$\frac{M_{1333}}{\Delta T} + P_{1333}$	$\frac{8}{175}$	0	0	$-\frac{16}{245}$	0
m=2, n=2			$\frac{M_{2222}}{\Delta T} + P_{2222}$	$-\frac{44}{315}$	$-\frac{4}{63}$	0	$\frac{44}{175}$	$\frac{M_{2242}}{\Delta T} + P_{2242}$	$\frac{4}{105}$	$\frac{44}{441}$	0	$-\frac{12}{175}$
m=3, n=1				$\frac{M_{3131}}{\Delta T} + P_{3131}$	0	$-\frac{88}{1575}$	0	$\frac{184}{945}$	$\frac{M_{3151}}{\Delta T} + P_{3151}$	0	$\frac{368}{4725}$	0
m=1, n=5					$\frac{M_{1515}}{\Delta T} + P_{1515}$	$-\frac{8}{27}$	0	$\frac{8}{441}$	0	$\frac{M_{1535}}{\Delta T} + P_{1535}$	$\frac{16}{189}$	0
m=2, n=4						$\frac{M_{2424}}{\Delta T} + P_{2424}$	$-\frac{88}{245}$	0	$\frac{8}{525}$	$\frac{88}{189}$	$\frac{M_{2444}}{\Delta T} + P_{2444}$	$\frac{24}{245}$
m=3, n=3							$\frac{M_{3333}}{\Delta T} + P_{3333}$	$-\frac{184}{525}$	0	0	$\frac{368}{735}$	$\frac{M_{3353}}{\Delta T} + P_{3353}$
m=4, n=2			Symmetry					$\frac{M_{4242}}{\Delta T} + P_{4242}$	$-\frac{520}{2079}$	$-\frac{184}{1323}$	0	$\frac{104}{231}$
m=5, n=1									$\frac{M_{5151}}{\Delta T} + P_{5151}$	0	$-\frac{208}{2079}$	0
m=3, n=5										$\frac{M_{3535}}{\Delta T} + P_{3535}$	$-\frac{368}{567}$	0
m=4, n=4											$\frac{M_{4444}}{\Delta T} + P_{4444}$	$-\frac{1040}{1617}$
m=5, n=3												$\frac{M_{5353}}{\Delta T} + P_{5353}$

$= 0$

(B-7)

$m \pm n$ = odd (antisymmetric buckling) (2S2C)

$A_{kl} \rightarrow$	A_{12}	A_{21}	A_{14}	A_{23}	A_{32}	A_{41}	A_{16}	A_{25}	A_{34}	A_{43}	A_{52}	A_{61}	
m=1, n=2	$\frac{M_{1212}}{\Delta T} + P_{1212}$	$-\frac{4}{45}$	0	$\frac{4}{25}$	$\frac{M_{1232}}{\Delta T} + P_{1232}$	$\frac{8}{315}$	0	$\frac{4}{63}$	0	$-\frac{8}{175}$	0	$\frac{4}{945}$	
m=2, n=1		$\frac{M_{2121}}{\Delta T} + P_{2121}$	$-\frac{8}{225}$	0	$\frac{44}{315}$	$\frac{M_{2141}}{\Delta T} + P_{2141}$	$-\frac{4}{175}$	0	$\frac{88}{1575}$	0	$-\frac{4}{105}$	0	
m=1, n=4			$\frac{M_{1414}}{\Delta T} + P_{1414}$	$-\frac{8}{35}$	0	$\frac{16}{1575}$	0	$\frac{8}{27}$	$\frac{M_{1434}}{\Delta T} + P_{1434}$	$\frac{16}{245}$	0	$\frac{8}{4725}$	
m=2, n=3				$\frac{M_{2323}}{\Delta T} + P_{2323}$	$-\frac{44}{175}$	0	$-\frac{4}{45}$	0	$\frac{88}{245}$	$\frac{M_{2343}}{\Delta T} + P_{2343}$	$\frac{12}{175}$	0	
m=3, n=2					$\frac{M_{3232}}{\Delta T} + P_{3232}$	$-\frac{184}{945}$	0	$-\frac{44}{441}$	0	$\frac{184}{525}$	$\frac{M_{3252}}{\Delta T} + P_{3252}$	$\frac{172}{3465}$	
m=4, n=1						$\frac{M_{4141}}{\Delta T} + P_{4141}$	$\frac{8}{1225}$	0	$-\frac{368}{4725}$	0	$\frac{520}{2079}$	$\frac{M_{4161}}{\Delta T} + P_{4161}$	$= 0$
m=1, n=6							$\frac{M_{1616}}{\Delta T} + P_{1616}$	$-\frac{4}{11}$	0	$\frac{8}{315}$	0	$\frac{4}{3675}$	
m=2, n=5			Symmetry					$\frac{M_{2525}}{\Delta T} + P_{2525}$	$-\frac{88}{189}$	0	$\frac{4}{147}$	0	
m=3, n=4									$\frac{M_{3434}}{\Delta T} + P_{3434}$	$-\frac{368}{735}$	0	$\frac{344}{17325}$	
m=4, n=3										$\frac{M_{4343}}{\Delta T} + P_{4343}$	$-\frac{104}{231}$	0	
m=5, n=2											$\frac{M_{5252}}{\Delta T} + P_{5252}$	$-\frac{1180}{3861}$	
m=6, n=1												$\frac{M_{6161}}{\Delta T} + P_{6161}$	

(B-8)

REFERENCES

1. Gowda, R. M. Siddaveere and K. A. V. Pandalai, *Thermal Buckling of Orthotropic Plates*, Studies in Structural Mechanics, Hoff's 65th Anniversary Volume, Indian Institute of Technology, Madras-36, India, 1970, pp. 9–44.

2. Tauchert, T. R. and N. N. Huang, "Thermal Buckling and Postbuckling Behavior of Antisymmetric Angle-Ply Laminates," Proc. Internat'l Symp. Composite Materials and Structures, Beijing, China, June 1986, pp. 357–362.

3. Tauchert, T. R. and N. N. Huang, "Thermal Buckling of Symmetric Angle-Ply Laminated Plates," *Composite Structures*, I. H. Marshall-editor, Elsevier Applied Science, London, 1987, pp. 1424–1435.

4. Thangaratnam, Kari R., Palaninathan, and J. Ramachandran, "Thermal Buckling of Composite Laminated Plates," *Computers and Structures*, Vol. 32, No. 5, 1989, pp. 1117–1124.

5. Huang, N.N. and T.R. Tauchert, "Postbuckling Response of Antisymmetric Angle-Ply Laminates to Uniform Temperature Loading," *Acta Mechanica*, Vol. 72, 1988, pp. 173–183.

6. Tauchert, Theodore R., "Thermal Stresses in Plates—Statical Problems," in *Thermal Stresses I*, Vol. 1, Elsevier Sciences Publishing Co., New York, 1986, pp. 23–141.

7. Ko, William L. and Raymond H. Jackson, *Thermal Behavior of a Titanium Honeycomb-Core Sandwich Panel*, NASA TM-101732, 1991.

8. Ko, William L. and Raymond H. Jackson, "Combined Compressive and Shear Buckling Analysis of Hypersonic Aircraft Structural Sandwich Panels," AIAA Paper No. 92-2487-CP. Presented at the 33rd AIAA/ASME/ASCE/AHS/ASC Structures, Structural Dynamics and Materials Conference, Dallas, Texas, April 13–15, 1992; also NASA TM-4290, 1991.

9. Ko, William L. and Raymond H. Jackson, *Combined-Load Buckling Behavior of Metal-Matrix Composite Sandwich Panels Under Different Thermal Environments*, NASA TM-4321, 1991.

10. Ko, William L. and Raymond H. Jackson, "Compressive and Shear Buckling Analysis of Metal Matrix Composite Sandwich Panels under Different Thermal Environments," *Composite Structures*, Vol. 25, July 1993, pp. 227–239.

11. Ko, William L., "Mechanical and Thermal Buckling Analysis of Sandwich Panels Under Different Edge Conditions," *Proc. 1st Pacific International Conference on Aerospace Science and Technology*, Tainan, Taiwan, Dec. 6–9, 1993.

12. Ko, William L. and Raymond H. Jackson, *Mechanical and Thermal Buckling of Rectangular Sandwich Panels Under Different Edge Conditions*, NASA TM-4535, 1994.

13. Tenney, D. R., W. B. Lisagor, and S. C. Dixon, "Materials and Structures for Hypersonic Vehicles," *J. Aircraft*, Vol. 26, no. 11, Nov. 1989, pp. 953–970.

14. Thornton, Earl A. “Thermal Buckling of Plates and Shells,” Applied Mechanics Review, Vol. 46, No. 10, October 1993, pp. 485–506.

15. Whetstone, W. D., *SPAR Structural Analysis System Reference Manual, System Level 13A, Vol. 1, Program Execution*, NASA CR-158970-1, Dec. 1978.

16. Ko, William L. “Thermocryogenic Buckling and Stress Analyses of 9 Partially Filled Cryogenic Tank Subjected to Cylindrical Strip Heating,” *Proceedings of 2nd Thermal Structures Conference*, Charlottesville, Virginia, Oct. 18–20, 1994. Also, NASA TM-4579, Oct. 1994.

REPORT DOCUMENTATION PAGE

Form Approved
OMB No. 0704-0188

1. AGENCY USE ONLY (Leave blank)	2. REPORT DATE	3. REPORT TYPE AND DATES COVERED
	May 1995	Technical Memorandum

4. TITLE AND SUBTITLE

Predictions of Thermal Buckling Strengths of Hypersonic Aircraft Sandwich Panels Using Minimum Potential Energy and Finite Element Methods

5. FUNDING NUMBERS

WU 505-70-63

6. AUTHOR(S)

William L. Ko

7. PERFORMING ORGANIZATION NAME(S) AND ADDRESS(ES)

NASA Dryden Flight Research Center
P.O. Box 273
Edwards, California 93523-0273

8. PERFORMING ORGANIZATION REPORT NUMBER

H-2009

9. SPONSORING/MONITORING AGENCY NAME(S) AND ADDRESS(ES)

National Aeronautics and Space Administration
Washington, DC 20546-0001

10. SPONSORING/MONITORING AGENCY REPORT NUMBER

NASA TM-4643

11. SUPPLEMENTARY NOTES

12a. DISTRIBUTION/AVAILABILITY STATEMENT

Unclassified—Unlimited
Subject Category 39

12b. DISTRIBUTION CODE

13. ABSTRACT (Maximum 200 words)

Thermal buckling characteristics of hypersonic aircraft sandwich panels of various aspect ratios were investigated. The panel is fastened at its four edges to the substructures under four different edge conditions and is subjected to uniform temperature loading. Minimum potential energy theory and finite element methods were used to calculate the panel buckling temperatures. The two methods gave fairly close buckling temperatures. However, the finite element method gave slightly lower buckling temperatures than those given by the minimum potential energy theory. The reasons for this slight discrepancy in eigensolutions are discussed in detail. In addition, the effect of eigenshifting on the eigenvalue convergence rate is discussed.

14. SUBJECT TERMS

Different edge conditions, Finite element method, Minimum potential energy theory, Sandwich panels, Thermal bucklings

15. NUMBER OF PAGES

54

16. PRICE CODE

A04

17. SECURITY CLASSIFICATION OF REPORT	18. SECURITY CLASSIFICATION OF THIS PAGE	19. SECURITY CLASSIFICATION OF ABSTRACT	20. LIMITATION OF ABSTRACT
Unclassified	Unclassified	Unclassified	Unlimited